Order Number 9224812

The molecular and biochemical analysis of alpha-galactosidase A activity variants

Fitzmaurice, Thomas Francis, Ph.D.

City University of New York, 1992

U·M·I
300 N. Zeeb Rd.
Ann Arbor, MI 48106

THE MOLECULAR AND BIOCHEMICAL ANALYSIS OF ALPHA-GALACTOSIDASE A ACTIVITY VARIANTS

by

THOMAS F. FITZMAURICE

A dissertation submitted to the Graduate Faculty in Biology
in partial fulfillment of the degree of Doctor of Philosophy,
The City University of New York

1992

This manuscript has been read and accepted for the Graduate Faculty in Biology in satisfaction of the dissertation requirement for the Degree of Doctor of Philosophy.

2/25/92
Date

Chair of Examining Committee
Prof. A. Henderson, Hunter College

4/1/92
Date

Executive Officer
Dr. Peter C. Chabora

Prof. P. Lipke, Hunter College

Thomas Schmidt-Glenewinkle
Prof. T. Schmidt-Glenewinkle, Hunter College

Prof. R. Desnick, Mt. Sinai

David F. Bishop
Prof. D. Bishop, Mt. Sinai

Prof. C. Eng, Mt. Sinai

Prof. M. Rattazzi, Cornell University
Supervisory Committee

The City University of New York

Abstract

THE MOLECULAR AND BIOCHEMICAL ANALYSIS OF
ALPHA-GALACTOSIDASE A ACTIVITY VARIANTS
by
Thomas F. Fitzmaurice

Adviser: Ann Henderson Ph.D.

Biochemical and molecular studies were carried out on the lysosomal hydrolase α-galactosidase A (E.C. 3.2.1.22, α-Gal A) in order to characterize variant enzyme activity. Determination of thermal stability, specific activity and enzyme kinetics was carried out on α-Gal A that had been partially purified from the lymphoblasts of an individual with residual enzyme activity as well as on enzyme from a high-activity variant exhibiting plasma enzyme activity levels of approximately 3 times the normal mean.

Characterization of α-Gal A from a residual activity variant revealed an enzyme with reduced thermostability and altered kinetic properties. This enzyme had half-lives of 11 and 8 minutes at 41 °C and pH 4.6 or 7.4, respectively, as compared to normal control values of 33 and 44 minutes under the same conditions. The K_m of the residual activity enzyme for 4-methylumbelliferyl-α-D-galactopyranoside (4-MU-α-Gal) was 4.1 mM as compared to 3.0 mM for the normal enzyme. The enzyme was also shown to have reduced affinity for the potent inhibitor, D-galacto-deoxynojirimycin, giving further evidence that the active site of the residual activity enzyme was altered. Molecular analysis of the residual activity allele revealed an A to G transition in exon 6 of the α-Gal A cDNA that resulted in the substitution of valine for methionine at residue 296 of the resulting protein (M296V).

Characterization of enzyme from the high-activity variant determined that its kinetic and physical properties were the same as those of normal enzyme. α-Gal A messenger RNA levels in the high-activity variant were also shown to be normal, indicating absence of increased transcription or stability. Sequence analysis of the high-activity allele revealed a G to A transition 30 nucleotides 5' of the translation start site in the cDNA. This mutation was inherited in an X-linked manner and also found in three additional, unrelated high-activity individuals thereby demonstrating its causative nature. *In vitro* transcription and translation of the normal and high-activity alleles resulted in normal levels of α-Gal A protein suggesting that some form of cell-specific regulation mechanism may be responsible for the increased amount of enzyme activity seen *in vivo*.

Dedication

This work is dedicated to my most important genetics "experiment" to date, my son Paul. May the wonder of his growth and development serve as a constant reminder of how little we really know of the processes that cause each of us to become unique individuals.

Acknowledgements

I would like to thank all of the people at Mount Sinai who had the pleasure of putting up with me during the course of this work, especially Dr. David F. Bishop. Most of all I would like to thank my wife, Carolyn, without whom I never would have even dreamed of trying something as crazy as this!

Preface

All of the experimental procedures described within this thesis were performed by the author with the following exceptions:

Lymphoblast cultures were established by Safiana Katz who also was responsible for maintaining lymphoblast and fibroblast cultures.

The initial cloning and sequencing of exon 6 from the residual activity variant and identification of the M296V mutation was performed by Christine Eng, M. D.

The identification and characterization of the defective enzyme caused by the N215S mutation was performed by David Bishop, Ph. D. and Cathy Painter and the point mutation was sequenced by Christine Eng, M. D.

SSCP analysis of the mother of one of the residual activity variants was performed by Lois Resnick-Silverman, Ph. D.

Table of Contents

List of Tables

List of Figures

List of Abbreviations

A	adenosine
ATP	adenosine triphosphate
C	cytosine
CAT	chloramphenicol acetyltransferase
cDNA	complementary DNA
Cer	ceramide
cpm	counts per minute
CTP	cytydine triphosphate
DAI	double-stranded RNA activated inhibitor
DEPC	diethylpyrocarbonate
DNA	deoxyribonucleic acid
DTT	dithiothreitol
EDTA	ethylenediaminetetraacetic acid
eIF	eukaryotic initiation factor
G	guanosine
Gal	galactose
α-Gal A	α-galactosidase A
α-Gal B	α-galactosidase B
ΔG	Gibbs free energy
GDP	guanosine diphosphate
Glc	glucose
GTP	guanosine triphosphate
HRI	hemin regulated inhibitor
HSA	human serum albumin
IRE	iron responsive element

IRE-BP	iron responsive element binding protein
kd	kilodalton
MES	[2-(N-morpholino) ethane-sulfonic acid]
Met-tRNA	methionine transfer RNA
min	minute
ml	milliliter
mRNA	messenger RNA
4-MU-α-Gal	4-methylumbelliferyl-α-D-galactopyranoside
PABP	poly(A) binding protein
PCR	polymerase chain reaction
RNA	ribonucleic acid
SDS	sodium dodecyl sulphate
Ser	serine
SSCP	single-strand conformation polymorphism
T	thymidine
U	uracil
uORF	upstream open reading frame

Chapter 1

Background

A. α-Galactosidase A and Fabry Disease:

α-Galactosidase A (E.C. 3.2.1.22, α-Gal A) is member of a class of proteins known as lysosomal hydrolases. Genetic deficiencies in these enzymes result in the different lysosomal storage diseases. To date, over thirty such diseases have been identified. The disease associated with α-Gal A deficiency is Fabry disease (1). In this disorder, deficient enzymatic activity causes neutral glycosphingolipids with terminal α-galactosyl moieties to accumulate in most visceral tissues and body fluids. Hemizygous males exhibit a characteristic skin lesion (angiokeratoma) as well as episodic crises of excruciating pain (acroparesthesias), corneal and lenticular opacities, reduced ability to sweat (hypohydrosis), and cardiac and renal dysfunction. If untreated by kidney dialysis or transplantation, death usually results from renal, cardiac or cerebral vascular complications with a mean life span of around forty years of age. Heterozygous females are typically asymptomatic except for corneal opacities and some angiokeratoma.

The earliest cases of Fabry disease were independently reported in 1898 by two dermatologists; Anderson in England, and Fabry in Germany (2,3). Anderson originally described a 39-year old male with proteinuria, finger deformities, varicose veins, and lymphedema. He suspected that the disease was a generalized disorder and because of the proteinuria suggested that abnormal vessels might be present in the kidneys as well as the skin. Fabry's original patient was a 13-year old male whom he followed for the next 30 years. He noted the presence of albuminuria, further described the cutaneous lesions noting the presence of small vessel aneurysm, and classified the dermatologic lesions as angiokeratoma corporsis diffusum. This designation is still used today.

Over the years the major clinical manifestations of the disease were characterized through the work of several different groups. In the early 1900's a hemizygous male was described as having anhydrosis and intermittent acroparesthesis that were aggravated by extremes in temperature (4,5). A skin biopsy from this individual revealed atrophy of the

sweat glands and aneurysmal dilation of the capillaries. The characteristic corneal opacities were first described in 1925 along with the vascular abnormalities in the conjunctiva and retina (6). In 1947, the first postmortem findings were reported in two affected brothers who died from renal failure (7). The presence of abnormal vacuoles in blood vessels were observed throughout their bodies thereby confirming that the disease was a generalized storage disorder. The nature of this disorder was further characterized in 1963 by Sweeley and Klionsky (8) who isolated and characterized two neutral glycosphingolipids, globotriaosylceramide (Gal-Gal-Glc-Cer) and galabiosylceramide (Gal-Gal-Cer), from the kidney of a Fabry hemizygote obtained at autopsy. Based on this finding they classified the disease as a sphingolipidosis. The X-linked inheritance of Fabry disease, which had been assumed for some time, was documented by analysis of a large pedigree in 1965 (9).

The nature of the enzyme defect in Fabry disease was determined in 1967 by Brady et al. (1). The defective enzyme, designated ceramide trihexosidase, was shown to be a lysosomal hydrolase required for the catabolism of globotriaosylceramide. The α-anomeric specificity of the galactosyl hydrolase was demonstrated through the use of artificial substrates (10). It was recognized shortly thereafter that there were two different enzymes, designated α-galactosidase A and B (α-Gal A and α-Gal B), that hydrolyzed synthetic substrates having terminal α-galactosyl moieties. Characterization of the two "isozymes" soon revealed several distinguishing characteristics of each form. α-Gal A was heat-labile while α-Gal B was able to retain up to 80% of its activity even after 4 hours at 50 $^{\circ}$C (11-14). The two forms could be distinguished immunologically (13,14) and could be separated by starch and cellulose acetate electrophoresis (14,15), isoelectric focusing (16-18), and ion exchange chromatography (13,19). These studies revealed multiple forms of α-Gal A with pI values ranging from 4.3 to 5.1 while α-Gal B had a single form with a pI of about 4.5. Neuraminidase treatment converted the multiple α-Gal A forms to a single band at pI 5.1 while the migration of α-Gal B was unaffected (20,21). This was initially thought to indicate that α-Gal A was a sialated form of the B isozyme. However, it was

clearly shown that it was only the heat-labile form (α-Gal A) that was deficient in Fabry disease and that any residual activity seen in classic hemizygotes could be precipitated with antibodies specific for α-Gal B. Inhibition studies indicated that α-Gal A was selectively inhibited by myoinositol while α-Gal B was strongly inhibited by N-acetylgalactosamine (11,12,14,15). α-Gal B also had a much higher affinity for nitrophenyl-α-N-galactosamine substrates (K_m=1 mM) than it did for nitrophenyl-α-D-galactoside analogs (K_m=20 mM) (11,12). This information suggested that the two forms were distinct enzymes and that α-Gal B was in actuality an α-N-acetylgalactosaminidase that had low affinity for artificial α-galactoside substrates. This was confirmed using natural substrates and the two genes were subsequently mapped to separate chromosomes;α-Gal B to 22q13 → 22qter (22) and α-Gal A to Xq21.33 → Xq22 (23).

B. α-Galactosidase A Activity Variants:

The basis for the biological activity of α-Gal A is derived from the specific three dimensional conformation it assumes upon folding. While it is generally accepted that this "native" conformation is determined by the linear sequence of amino acid residues present in the polypeptide chain, the conversion of this sequence into a functioning three dimensional structure is still not well understood. In particular, the structural basis for such properties as stability, substrate specificity, mechanism of catalysis, and subunit interaction remain unclear. Advances in DNA technology have now made it possible to study these structure-function relationships by site-directed mutagenesis of specific amino acid residues. Because this approach allows for the introduction of side chains that vary in volume, charge, hydrogen-binding capability, and hydrophobicity, the influence of each of these properties on enzyme function can be tested. While this method is powerful it can also be time-consuming since there is often no *a priori* method for choosing the residue to be mutated. A more direct approach to the study of structure-function relationships is the

analysis of phenotypic variants that occur either naturally or as the result of randomly induced mutations. Individuals with variant α-Gal A activity represent a set of naturally occurring phenotypic mutations. These variants include atypical hemizygotes that have sufficient residual activity to prevent them from exhibiting classical symptoms (24-29) as well as individuals whose activity is 2 to 3 times above normal levels (unpublished observation). Characterization of the protein present in several residual activity variants has revealed the presence of enzymes with altered stability, altered processing and/or altered substrate affinity (24-30). These individuals are not only important as examples of the heterogeneity of mutations that give rise to Fabry disease but also for the opportunity they provide to study the structure-function relationships of α-Gal A. Isolation and sequencing of the gene encoding α-Gal A (31-34) has made it possible to determine the precise cause of variant activity at the molecular level. The first such molecular demonstration of residual activity was initially detected as an *Msp* I restriction site obliteration and subsequently shown to be a C to T transition (24).

C. Peptide Chain Initiation:

The underlying mechanism that results in the increased α-Gal A activity discussed in this paper involves an increase in the translational efficiency of the α-Gal A messenger RNA. The translational efficiency of any message is primarily determined by the rate at which it initiates protein translation. Therefore, in order to understand the mechanism responsible for increased α-Gal A activity, it is important to have an overall understanding of the process of peptide chain initiation.

The initiation of protein translation is a complicated process that involves the interaction of 25 or more initiation factors and their cofactors (35). Although much work has been done in the past decade, our overall understanding of this process is far from complete. The complexity of the process stems from the fact that, unlike prokaryotes, eukaryotic mRNAs do not contain a highly conserved recognition sequence in their 5'

leader sequence that interacts with the ribosomal subunits to initiate formation of the active translation complex. Eukaryotic mRNA's must instead compete with each other for a limiting set of factors that are responsible for the proper assembly of the translational apparatus. This process can be broken down into a series of discrete steps. The first of these consists of the binding of Met-tRNA to the 40S ribosomal subunit to form the preinitiation complex. This complex joins with the messenger RNA to form the initiation complex and then migrates along the mRNA template until it reaches the AUG initiation codon. The 60S ribosomal subunit then binds thereby completing the formation of the 80S translation complex. Either this process as a whole, or one of its individual steps, provides a discriminatory mechanism that enable different mRNAs to be translated with different efficiencies.

The first step of the initiation process is the binding of Met-tRNA to the 40S subunit to form the pre-initiation complex (Figure 1). This step is carried out by eukaryotic initiation factor 2 (eIF-2), a multisubunit protein which, when bound to GTP, binds Met-tRNA to form a ternary complex. This binding has been shown to be inhibited by mRNA unless a cofactor (eIF-2C) is present (36) and may also be inhibited by the binding of ATP by eIF-2 (37). The formation of the ternary complex is also sensitive to the energy state of the cell since eIF-2 binds GDP 400-fold more tightly than it does GTP (38).

The binding of the mRNA to the preinitiation complex is preceded by the binding of several initiation factors to the mRNA itself. These include eIF-4A, a 46 kd RNA dependent ATPase with helicase activity, eIF-4B, an 80 kd RNA binding protein that stimulates the action of eIF-4A and eIF-4F (also known as the cap-binding complex). eIF-4F is a multisubunit protein that contains cap binding specificity (25 kd subunit, also known as eIF-4E, eIF-4α or cap-binding protein), a subunit with ATPase and helicase activity (46 kd subunit), plus a 220 kd subunit (eIF-4γ). Although the function of the 220 kd subunit is unknown, its importance has been demonstrated by studies of poliovirus infected cells in which the 220 kd subunit is cleaved and cap-specific translation is rendered

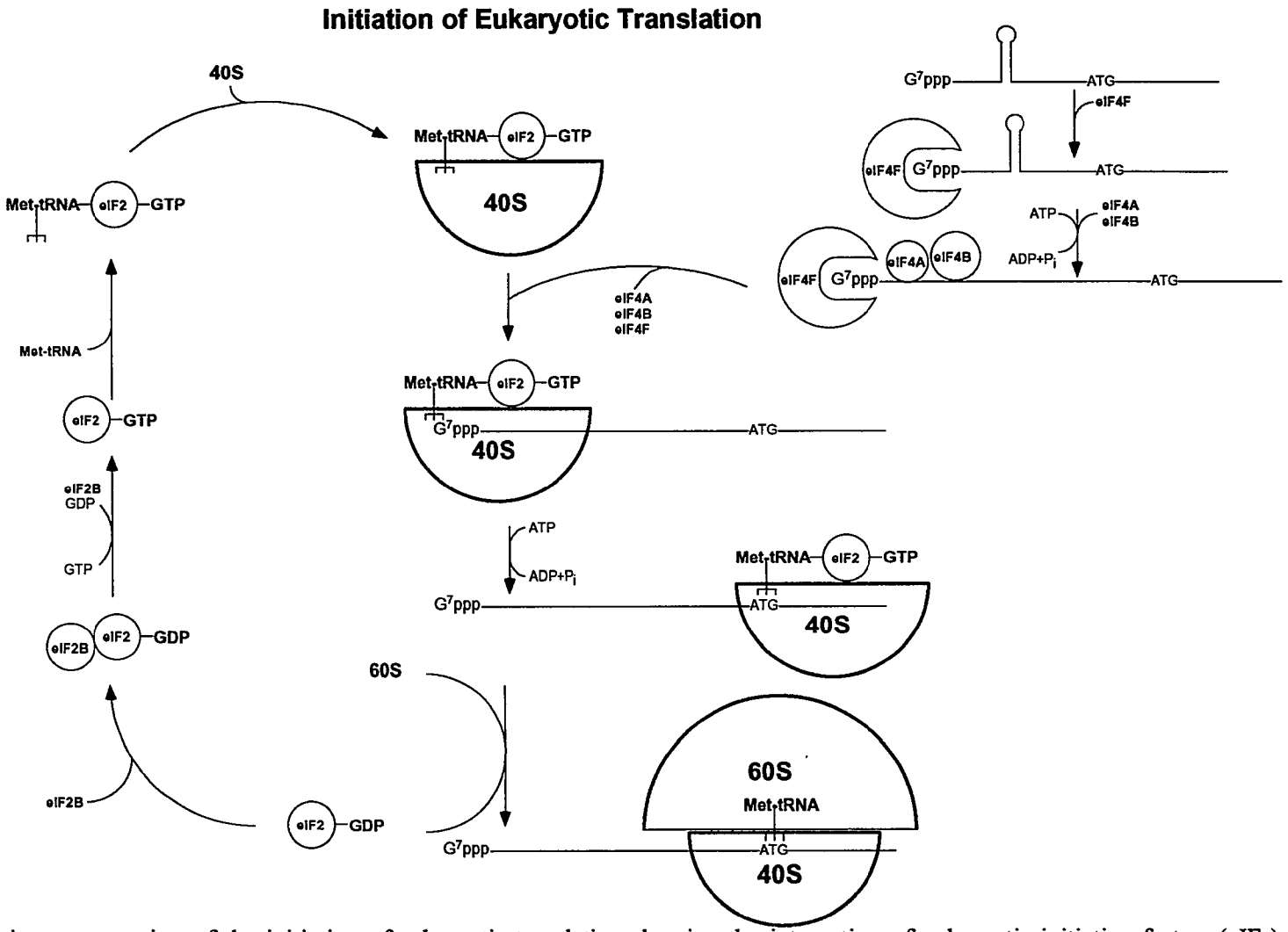

Figure 1: Schematic representation of the initiation of eukaryotic translation showing the interaction of eukaryotic initiation factors (eIFs), mRNA and the 40S and 60S ribosomal subunits that lead to the formation of the 80S translation complex.

inactive (39). It may therefore function to maintain the 25 kd subunit in an optimal conformation for cap binding. It is generally believed that the 46 kd subunit of eIF-4F is a complexed form of eIF-4A.

The action of these factors is thought to initiate with binding of eIF-4F to the 5' methylguanosine cap structure in an ATP-independent manner via the 25 kd subunit followed by the binding of eIFs 4A and 4B (Figure 1). The helicase activity of eIF-4A is then utilized in an ATP-dependent manner to melt secondary structure in the vicinity of the cap structure thereby allowing the 40S-eIF-2-GTP-Met-tRNA preinitiation complex to bind in order to form the initiation complex. This destabilization of the mRNA secondary structure in the vicinity of the cap structure is known to be important since mRNAs lacking any significant secondary structure exhibit high degrees of initiation complex formation and translation even in the absence of a functional cap-binding complex (40,41). In addition to this, a moderately-stable stem-loop structure (ΔG=-30 kcal) located within 12 bases of the cap site has been shown to strongly inhibit translation whereas the same structure, when located further downstream, has no effect (42). Although the mechanism of the binding of the messenger RNA to the preinitiation complex is not known, there is recent evidence to suggest that it may involve eIF-2's ability to bind mRNA and ATP (37). The proposed mechanism is that ATP binds to the eIF-2-GTP-Met-tRNA ternary complex thereby causing a conformational change that causes the Met-tRNA to be released and allowing eIF-2 to bind to the mRNA.

Once the 40S ribosomal subunit has bound to the mRNA it migrates in a 3' direction in search of the AUG initiation codon. That the initiation complex actually travels along the mRNA as opposed to jumping to the AUG initiation codon has been shown in studies designed to block this scanning process. Although the migrating complex has been shown to be capable of traversing stem-loop structures with a ΔG of -30 kcal, introduction of a more stable structure of ΔG=-50 kcal or more has been shown to trap the 40S subunit in the 5' leader sequence (42-46). Likewise, hybridization of an oligonucleotide

complementary to the 5' leader sequence has also been shown to block migration of the initiation complex (47). Both of these methods inhibit translation of a particular mRNA even though the introduced secondary structure does not include the AUG initiation codon. This demonstrates that the 40S ribosomal subunit must traverse the 5' leader sequence of the mRNA before translation can begin. There have been several reported cases of "internal initiation" of ribosomes in viral mRNAs (48-53) but these appear to be unique cases and have not been seen in eukaryotic translation.

The criteria for selecting the proper initiation codon appears to reside in the context of the sequence and secondary structure surrounding the AUG as well as its position relative to the cap structure. The established consensus sequence for initiation is GCC(A/G)CCATGG with the presence of a purine, preferentially an A, at the -3 position being of utmost importance (54-60). In the event that a pyrimidine or a G occupies the -3 position, the remaining positions take on increased importance, especially the G residue at +4. When the scanning 40S subunit encounters an AUG in the proper context it presumably pauses and this allows the 60S ribosomal subunit to bind with the subsequent release of the initiation factors. eIF-2 is released in a complex with GDP and must be phosphorylated before it is once again active. This reaction is carried out by eIF-2B (guanosine exchange factor or GEF) which catalyzes a phosphate exchange reaction with free GTP to recharge the complex (38). The factors responsible for the recognition of the AUG codon and the consensus sequence surrounding it are unknown. This process can be aided by mRNA secondary structure located immediately downstream from the initiator AUG that acts to increase the length of time that the 40S subunit remains stalled at the initiator AUG (61).

If a migrating 40S subunit encounters an AUG codon in a less than favorable context it may pass over this codon and continue to scan downstream. All of the rules on consensus sequences and secondary structure notwithstanding, the bottom line is that, in

greater than 90% of eukaryotic mRNAs looked at to date, the first AUG encountered by the migrating complex acts as the initiation codon (56,57,62).

The initiation of translation, as described above, can be regulated by a number of different methods including the action of small upstream open reading frames (uORFs), specific interaction of secondary structure in the mRNA 5' leader sequence with regulatory factors, phosphorylation of initiation factors, or possibly even some form of interaction with the poly(A) tail of the mRNA.

The effect of uORFs is generally an inhibitory one and has been examined by several groups (63-73). The findings indicate that the effect of an uORF on translation is dependent on both its position relative to the 5' cap structure as well as the distance between its termination codon and the initiation codon of the mRNA being studied. uORFs that begin within 10 nucleotides of the 5' cap structure appear to have little or no effect on translation initiation whereas when positioned 44 nucleotides from the cap structure the same uORF has an inhibitory effect (71). This effect is most likely caused by scanning ribosomes ignoring AUG codons that occur too close to the cap structure and thereby rendering the more 5' uORF inactive. The inhibitory effect of uORFs is also modulated by the distance between their termination codon and the AUG codon at which the ribosomes must reinitiate for proper translation to take place. This effect has been shown to decrease as the uORF is moved further upstream from the initiator AUG and has no effect on translation once a distance of 79 nucleotides between the two reading frames had been reached (66). The probable cause of this effect is that once termination has occurred at the uORF, the 40S ribosomal subunit is lacking the eIFs and Met-tRNA necessary to reinitiate translation at a downstream AUG. The longer the distance is before the next AUG is reached, the more time there is for the components of the initiation complex to reassemble.

The most extensively studied example of the regulation of translation through reinitiation is the yeast GCN4 mRNA (64,67-69,72,73). This message, which encodes a transcriptional activator of amino acid biosynthetic genes, contains 4 small uORFs in its 5'

leader sequence which control its translation according to the cell's biosynthetic needs. Under normal growth conditions translation initiation at the uORFs inhibits translation from the GCN4 AUG presumably because the the 40S subunit does not have enough time to associate with the required factors after terminating translation of the fourth uORF for reinitation to occur. Under conditions of amino acid starvation, however, the concentration of the necessary factors is reduced such that after termination of the first and second uORFs the reinitiation complex is not formed in time to translate the third and or fourth uORF and instead reinitiates at the GCN4 AUG. It has been shown that the two most 5' uORFs can be replaced with unrelated uORFs without any effect but it appears that sequences 3' to the stop codon of uORF4 may also play a role in the regulatory process (72).

A second possible method of translational regulation is the interaction of a specific binding protein with a region of secondary structure contained within the 5' leader sequence of an mRNA. This has been shown to be the case in the regulation of the iron-sequestering protein, ferritin. Analysis of the 5' leader sequence of ferritin mRNA from several different species has revealed the presence of a moderately stable stem-loop structure, known as the iron-responsive element (IRE), located 33-39 nucleotides from the 5' cap structure (74). Although the stability of this structure is not great enough to inhibit translation on its own, upon the binding of a 90 kd IRE-binding protein (IRE-BP) the translation of ferritin mRNA is inhibited. The cellular concentration of the IRE-BP reflects the cellular iron concentration thereby making the system sensitive to changing conditions. The effectiveness of this structure, as with the other secondary structures, is dependent on its position relative to the 5' cap structure. If the IRE is moved further downstream from the cap, its ability to regulate ferritin translation is reduced. The IRE has also been found in the 5' untranslated sequence of erythroid ALA-synthase and aconitase mRNAs as well as in the 3' untranslated region of the message for the transferrin receptor (75). This indicates that protein-mRNA interactions of this type are an integral part of the regulation of proteins involved in iron metabolism. Many other mRNAs examined to date have been shown to

contain moderately stable stem-loop structures in their 5' untranslated sequence. It is not difficult to envision a family of proteins that could down-regulate translation of these messages by stabilizing these structures by binding to them. Alternatively, the translation of mRNAs containing strong inhibitory stem-loop structures in their leader sequences could be increased through the binding of proteins that could "melt" such structures.

As with many other cellular processes, phosphorylation plays a major role in the regulation of the initiation of protein synthesis. This regulation can be either positive or negative depending on the targeted initiation factor. Many proteins involved in the translation process have been shown to undergo phosphorylation but only a few of these have been studied in detail. Of these, the most important appear to be eIF-4F, eIF-4B and eIF-2. eIF-4F has been shown to undergo phosphorylation of both the α (25 kd, eIF-4E) and γ (220 kd) subunits (76,77). The dephosphorylation of the α subunit has been shown to lead to a decrease in protein synthesis in response to heat shock or during meiosis. Expression of mutated eIF-4E in which the phosphorylated residue, Ser^{53}, has been changed to an alanine has shown that phosphorylation is necessary for association with the preinitiation complex to occur. Additional studies have shown that overexpression of of eIF-4E in NIH3T3 cells causes malignant transformation to occur while overexpression of the Ala^{53} mutant has no effect (78). These studies show that eIF-4E plays an important role in the regulation of the cell growth cycle and that its action is regulated by phosphorylation. The sites of phosphorylation of the 220 kd subunit and the effects that it has on translation have not yet been determined. eIF-4B undergoes phosphorylation at multiple sites and partial dephosphorylation occurs during heat shock and serum deprivation (79,80). There is, however, no direct evidence that phosphorylation of eIF-4B has any effect on translation.

The main site of translational control by phosphorylation appears to be the α subunit of eIF-2. The step at which this phosphorylation exerts its effect seems to be during the recycling of the eIF-2-GDP complex since phosphorylation of eIF-2-GTP-Met-

tRNA complexes does not inhibit interaction with the 40S ribosomal subunit (81). During the recycling process, phosphorylated eIF-2-GDP complexes bind eIF-2B but the phosphate exchange reaction does not take place (38). This effectively sequesters eIF-2B making it unavailable to recycle nonphosphorylated complexes. Since eIF-2B is present at much lower concentrations than eIF-2, phosphorylation of only 30% of the eIF-2s severely inhibits protein synthesis. Kinases specific for the α subunit of eIF-2 have been shown to act in response to hemin starvation (hemin regulated inhibitor or HRI) or to the presence of double-stranded RNA (double-stranded RNA activated inhibitor or DAI) (82-84). Interestingly, eIF-2B has also been shown to undergo phosphorylation (85). This modification, which increases its activity, may provide a means to balance the negative effect that phosphorylation of eIF-2 has on its activity.

Recent studies have provided evidence that translational efficiency may be modulated by the poly(A) tail located at the 3' end of the mRNA. In one set of such studies mRNAs whose poly(A) tails had been removed were shown to translate only half as well as their polyadenylated counterparts (86). This phenomenon was also shown to be directly related to the length of the poly(A) tail in that translation increased as the length of the tail increased from 5 to 32 adenylate residues. This difference in translational efficiency was shown to take place at the level of initiation since deadenylated messages were found associated with 80S ribosomal complexes only half as often as mRNAs possessing poly(A) tails. Translation was also shown to be inhibited by exogenously added poly(A), giving further evidence that some type of interaction was occurring between poly(A) and the translational machinery. The poly(A) binding protein (PABP) may also have a role in this mechanism in that inhibition by exogenously added poly(A) was reversed by the addition of PABP. Recent studies in yeast have supported this by revealing that lethal mutations in the PABP gene can be reversed by mutations in the 60S ribosomal subunit (87). Other studies have concluded that the poly(A) tail increases the translation of messenger RNA by causing reinitiation of translation of that mRNA to occur more frequently (88). It has also

been shown that mRNAs injected into *Xenopus* oocytes are translated more efficiently if they are polyadenylated (89,90). In all of the studies mentioned above the effect of polyadenylation on translational efficiency was carefully shown not to be an artifact of mRNA stability. If the poly(A) tail does have a role in translation it is not likely to be a universal one since there are several known cases of translationally inactive polyadenylated mRNAs as well as messages whose poly(A) tails become shortened as they become translationally active (88).

Specific instances of the translational control of protein expression have been documented in several different cell types. The most extensively studied system is the *Xenopus laevis* oocyte in which maternally derived mRNAs are differentially translated during the early stages of embryogenesis (91). This process has been demonstrated by microinjecting CAT constructs that differ only by the presence or absence of a stable stem-loop structure in the 5' leader sequence into *Xenopus* oocytes (92). Constitutively high levels of protein were translated from a construct lacking the 5' stem-loop while the construct containing the stem-loop was translated in a developmentally regulated manner. This type of experiment has also been performed using the 5' leader sequence of ribosomal protein S19 fused to CAT (93). In this case it was found that the 35 nucleotide long 5' leader sequence from S19 was sufficient to make CAT expression mimic that of ribosomal proteins *in vivo.*

Cell specific translational control has also been demonstrated in a rat pancreatic tumor and in rat skeletal muscle cells. In the tumor cells it has been shown that two highly homologous insulin genes exhibit a 10 fold difference in translational efficiency (94). This difference was no longer seen if the transcripts were capped *in vitro*, suggesting that the *in vivo* capping of one of the messages is deficient. In the rat muscle cells, translation of several muscle-specific messages was inhibited when cell fusion was blocked by EGTA treatment (95). This phenomenon, which presumably results from the interaction of some cell specific factor, was not reproducible in an *in vitro* system.

Significance:

The research described herein will increase our understanding of lysosomal enzymes and their associated storage diseases. The defective activity of α-Gal A results in Fabry disease (1). This enzymatic defect causes neutral glycosphingolipids with terminal α-galactosyl moieties to build up in body fluids and most visceral tissues (96). This disease represents an excellent model to investigate the effects that changes at the DNA level have on the structure and function of the corresponding protein. The study of the enzyme is facilitated by the fact that it functions as a homodimer (97) and exhibits X-linked inheritance (9). While the mode of inheritance causes complications in the diagnosis of heterozygotes due to lyonization, it greatly simplifies the characterization of males with variant activity since only one allele is present. A detailed characterization of α-Gal A in individuals with variant activity will not only provide an explanation for their altered activity but will also provide insight into the structure-function relationships present in the normal enzyme. Determining the cause of these changes at the DNA level may make it possible to modify normal α-Gal A in order to increase its activity and/or stability. Having the capability to perform such manipulations will allow for the production of an enzyme that is better suited for studies involving enzyme replacement therapy.

The first *in vitro* (98) and *in vivo* (99) therapeutic trials of α-Gal A replacement took place in the early 1970's. These studies, along with subsequent trials (100), demonstrated the effect that the direct administration of enzyme could have on accumulated substrate levels. By injecting hemizygotes with purified α-Gal A over a four month period it was shown that not only could substrate be depleted from the circulation, but that the accumulated substrate could be mobilized from cellular sites of deposition as well. These studies were discontinued due to a lack of purified enzyme. Recombinant DNA techniques now have made it possible to produce large amounts of α-Gal A with which to continue these studies. These advances along with a better understanding of the structural

determinants of stability and substrate affinity will hopefully make enzyme replacement therapy in Fabry disease a reality in the not too distant future.

Chapter 2

Molecular and Biochemical Analysis of Residual Activity Variants

A. Introduction:

The deficient activity of the lysosomal hydrolase α-Galactosidase A (α-Gal A) results in Fabry disease (1). The major clinical manifestations of this X-linked disorder are caused by the accumulation of neutral glycosphingolipids with terminal α-galactosyl residues in vascular endothelial and smooth muscle cells. The onset of the disease is usually in childhood or adolescence and is marked by a characteristic skin lesion (angiokeratoma) as well as episodic crises of excruciating pain (acroparesthesias), corneal and lenticular opacities, reduced ability to sweat (hypohydrosis), and cardiac and renal dysfunction. Death usually results from renal, cardiac or cerebral vascular complications with a mean life span of around forty years of age.

A growing number of cases have been identified in which the major manifestations of Fabry's disease are confined to the myocardium. These cases have been discovered due to the onset of cardiac complications at an age at which typical hemizygotes would have passed away. Upon the death of several such individuals, autopsy analysis revealed the accumulation of globotriaosylceramide exclusively in the heart tissues of these individuals (101,102). Although α-Gal A activity assays were not performed on these individuals due to their asymptomatic nature, assays performed on female family members of a deceased patient suggested that enzyme activity levels were reduced (101).

Described here is a 54 year old male (patient PP) with residual α-Gal A activity ranging from 1 to 25% from various sources. This residual activity is sufficient to limit the disease manifestations to the myocardium (103). Biochemical and molecular studies were carried out on partially purified α-Gal A isolated from lymphoblasts of the variant patient with residual activity and a normal control. These studies were designed to characterize the thermal stability, specific activity and kinetics of the normal and variant enzymes.

A study in this laboratory designed to identify α-Gal A mutations was concurrent with this thesis research and focused on exons 5-7 of the α-Gal A gene. An A to G

transition was identified at nucleotide 886 of the α-Gal A cDNA from patient PP that resulted in the substitution of valine for methionine at residue 296 of the resulting protein (M296V) (103). Computer-assisted analysis of this mutation predicted that this substitution would convert a random coiled region of secondary structure into β-pleated-sheet motif. In this study, the remainder of the coding sequence of α-Gal A was sequenced in order to determine if any additional mutations were present, and the mutant enzyme was partially purified and characterized.

B. Materials and Methods:

α-Galactosidase A assays

The method of Desnick et al. (104) was used to determine α-Gal A activities in various sources with the following modifications. A stock solution of 5.0 mM 4-methylumbelliferyl-α-D-galactopyranoside (4-MU-α-Gal, Genzyme Corp, Cambridge, MA) containing 117 mM N-acetylgalactosamine (GalNAc, United States Biochemicals, Cleveland, OH) was prepared in 0.15 M citrate-phosphate buffer, pH 4.6 (105). The reaction mixture, containing 150 µl of substrate stock solution plus 10 to 25 µl of enzyme solution, was incubated for 10 to 120 min at 37 °C. The reaction was terminated by the addition of 2.3 ml of 0.1 M ethylenediamine and the amount of fluorescent product was determined using a Turner model 111 fluorometer (Sequoia-Turner, Mountain View, CA). For cell extracts, protein concentration was determined using the fluorescamine assay (106).

Partial Purification of α-Gal A from lymphoblast extracts

Approximately 10^8 lymphoblasts were harvested by centrifugation, washed with saline, and resuspended in 10 ml of 10 mM sodium phosphate, pH 6.5. Cells were subjected to three 10 second bursts in a Branson cup sonicator at 4 °C and the cell debris was removed by centrifugation at 12,000 X g for 15 min. The pH of the cell extract was adjusted to approximately 5.2 by adding one tenth volume of 1.0 M MES, pH 5.0, and then centrifuged at 5,000 X g for 15 min to remove any precipitate. The extract was next applied to a 1 ml α-Gal A affinity column (106) which was then washed with 5 ml of citrate-phosphate buffer, pH 4.6, containing 117 mM GalNAc and 1 mg/ml human serum albumin (HSA). α-Galactosidase A activity was eluted from the column with 4 ml of

citrate-phosphate buffer, pH 6.0, containing 0.4 M galactose and 1 mg/ml HSA. The eluate was concentrated to 1 ml using a Centricon 30 concentrator (Amicon, Beverly, MA) and desalted to 10 mM sodium phosphate, pH 6.5, containing 1 mg/ml HSA on a 0.75 X 18 cm column of Sephadex G50 medium mesh (Pharmacia, Piscataway, NJ). A purification done in the absence of HSA approximated the fold purification to be about 25.

Heat inactivation of α-Gal A

Fourteen units (U) of partially purified α-Gal A were diluted to 700 µl with HSA buffer (1 mg/ml HSA in 10 mM sodium phosphate, pH 6.5). To one half of this was added 58 µl of 1 M NaOAc, pH 4.56, and to the other half 42.5 µl of 1 M HEPES, pH 7.53, in order to adjust the pH of the sample to 4.6 or 7.4, respectively. Twenty five µl of each sample was then aliquoted in duplicate to 10 x 75 mm test tubes in an ice water bath using a Hamilton syringe. The tubes were covered and placed in a 40 °C water bath and duplicates removed to an ice water bath at 0, 5, 10, 15, 20, 30, and 45 min for pH 4.6 and 0, 5, 10, 20, 30, 45, and 60 min for pH 7.4. Each sample was then assayed for 2 hr as described.

K_m determination

Using a Hamilton syringe, 1.0 U of partially purified α-Gal A in 25 µl of HSA buffer was aliquoted in duplicate into 10 x 75 mm test tubes maintained in an ice water bath. Duplicate assays were performed for 2 hr using 8.0, 6.0, 4.0, 2.0, 0.8, 0.6, or 0.4 mM 4-MU-α-Gal containing 117 mM GalNAc. The K_m of the sample was determined from the Lineweaver-Burke plot (107).

Inhibition of the residual activity enzyme by D-galacto-deoxynojirimycin

The reaction was initiated by mixing, in duplicate on ice, 150 µl of either 5 or 2.5 mM 4MU-α-Gal A substrate, 17.5 µl of the appropriate 10X inhibitor solution and 1 U of partially purified α-Gal A in 7.5 µl of HSA buffer. The tubes were then assayed at 37 °C for 2 hours as described. The K_i was determined from the Dixon plot (107) of the resulting data.

Immunotitration of α-Gal A

The immunoprecipitation solutions were prepared with the sequential addition of 60 µl of HSA buffer, 1.0 U of partially purified α-Gal A in 10 µl HSA buffer, 10 µl of the appropriate antibody dilution, and 10 µl of whole rabbit serum diluted 1:20 in HSA buffer, to a microfuge tube in an ice water bath. A control reaction without the primary antibody was set up in order to determine the units of activity present per assay. The mixtures were incubated at 37 °C for 30 min and then 10 µl of goat anti-rabbit (BioRad, Melville, NY), diluted 1:4 in HSA buffer, was added to each tube. The tubes were incubated an additional 30 min at 37 °C and then overnight at 4 °C. The samples were then centrifuged at 12,000 X g for 15 min at 4 °C. The supernatants were removed to fresh tubes and the pellets were resuspended in 100 µl of HSA buffer and then centrifuged as before. This supernatant was discarded and the pellets were resuspended in 25 µl of HSA buffer. Activity assays were for 2 hr as described using 25 µl of the supernatant or pellet suspension. The percent activity remaining was determined as compared to the activity present in the control tubes.

Cloning and sequencing of the residual activity allele

Total RNA was isolated from lymphoblasts from the residual activity variant or a normal control (108). Ten micrograms of RNA was primed with oligo dT and reverse

transcribed for 1 hour at 37 °C in a 50 μl reaction containing 50 mM Tris-HCl (pH 8.3), 75 mM KCl, 3 mM $MgCl_2$, 10 mM DTT, 500 μM each dATP, dCTP, dGTP and dTTP, 50 μg/ml oligo dT and 10,000 u/ml reverse transcriptase. The entire α-Gal A cDNA was PCR amplified, from 10 μl of the first strand synthesis reaction, in two overlapping fragments by using two sets of primers. The first of these sets consisted of oligonucleotide 210 and oligonucleotide 173, which amplified nucleotides -20 to 836, and the second set contained oligonucleotide 153 and oligonucleotide 252, which amplified nucleotides 736 to 1385 (Table 1). PCR was carried out in a 100 μl reaction containing 50 mM KCl, 10 mM Tris-HCl (pH 9.0), 1.5 mM $MgCl_2$, 0.01% gelatin, 0.1% Triton X-100, 1 μg of each primer and 0.5 unit of Taq polymerase. Thirty cycles were carried out consisting of 1 min at 94 °C, 1 min at 55 °C and 1 min at 72 °C. The amplified products were digested with the appropriate restriction enzymes and ligated into pGEM-4Z that had been digested with the same enzymes. Double stranded template was isolated from the resulting clones and sequenced by the dideoxy chain termination method using the Sequenase kit (United States Biochemicals, Cleveland, OH) using both universal and α-Gal A specific primers.

For genomic sequencing, DNA was isolated from lymphoblasts (109) and exons 5 through 7 were amplified using oligonucleotide 187 and oligonucleotide 203 (Table 1). The amplified product was digested with *Hind* III and *Eco* RI and ligated into pGEM-4Z that had been similarly digested. Sequence analysis was carried out as described above.

Single Strand Conformation Polymorphism (SSCP) Analysis:

To detect point mutations in patient DNA, individual exons were amplified, denatured, and alterations in the mobility of the single strands were detected using non-denaturing sequencing gels. For example, exon 5 was PCR amplified using 100 ng of genomic DNA as template, 10 pmoles each of primers 187 and 276 (Table 1), 625 pmoles of each dNTP, 25 μCi each of ^{35}S dATP and dCTP, 5 μl of 10X Taq polymerase buffer

Oligonucleotide Number	5' Coordinate Genomic	cDNA	Sense	Sequence
210	1160	-20	+	5'-ACTACTGAATTC|GCTGTCCGGTCACCGTG-3'
173	10232	817	-	5'-ATGTACGTCGAC|AGATGTCCAGTCCAAGATAC-3'
153	10133	736	+	5'-ACTACTGAGCTC|CAATTATACAGAAATCCGACAGT-3'
252	11268	1366	-	5'-GCGGAATTC|TCGAGGGATCCTTAAAGTAAGTCTTTTAATG-3'
187	8600	—	+	5'-ATCATCGAGCTC|ACAAGGATGTTAGT-3'
203	11301	—	-	5'-ACTACTGAATTC|CAGGAAGTAGTAGTTGG-3'
276	10339	—	-	5'-ACTACTGAATTC|AACAAGCCTACCGCAGG-3'
274	10584	876	+	5'-TCCTTTATTCATGTCTAATGA-3'
275	10584	876	+	5'-TCCTTTATTCGTGTCTAATGA-3'
207	926	—	+	5'-ACTACTGAATTC|GGATCACTAAGGTGCCGC-3'
219	1460	—	-	5'-GCTGCTGAATTC|AACTGTTCCCGTTGAGACTC-3'
253	1140	-40	+	5'-GGTTACCCGCGGAAATTTATG-3'
254	1140	-40	+	5'-GGTTACCCGCAGAAATTTATG-3'
272	1106	-75	+	5'-GCCGCCATATGAGTGAATTGTAATACGACTCACTATAG|TTGGTCCGCCCCTGAGGT-3'
262	1306	110	-	5'-GCCG|CCATGGTAGGCGTCCTT-3'

Table 1: Oligonucleotides used for various studies listed by number, genomic coordinate (34), cDNA coordinate (32), sense and sequence. The nonhomologous 5' portion of the oligonucleotide containing restriction enzyme sites used for cloning (underlined) is separated from the 3' portion containing the α-Gal A sequence by a vertical line.

(500 mM KCl, 100 mM Tris-HCl pH 9.0, 15 mM $MgCl_2$, 0.1% gelatin, 1% Triton X-100) (Promega Biotech, Madison, Wisconsin), 2.5 units of Taq polymerase and H_2O to a final volume of 50 µl. PCR was carried out for 30 cycles consisting of 1 min at 94 °C, 1 min at 55 °C and 3 min at 72 °C. After the purity of the product from this reaction was confirmed by electrophoresis on a 1% agarose gel, the product was diluted 1:5 with 0.1% SDS, 10 mM EDTA. Four microliters of this dilution was added to 4 µl of sequence stop buffer (95% formamide, 0.33% xylene cyanol, 0.33% bromophenol blue), denatured for 5 min at 95 °C and loaded onto a 6% acrylamide/bis non-denaturing gel containing 10% glycerol. Electrophoresis was at 95 milliamps for 6 hours at 4 °C after which the gel was dried and autoradiographed using Kodak Xomat AR film.

Allele-specific hybridization

Genomic DNA was isolated from lymphoblasts (109) and exons 5 through 7 were amplified using oligonucleotide 187 and oligonucleotide 203 (Table 1). One half of the PCR reaction (50 µl) was denatured by adjusting it to 0.4 M NaOH, 25 mM EDTA in a final volume of 400 µl.

A Zeta-Probe nylon membrane was cut to fit a dot blot apparatus (Schleicher and Schuell, Keene, NH) wet in boiling water and then soaked in 2X SSC (1X SSC is 0.15 M sodium chloride, 0.015 M sodium citrate) for 20 min along with a piece of Whatman 3MM filter paper. The filter paper and membrane were assembled into the dot-blot apparatus and each well washed under vacuum with 100 µl of 10X SSC. The denatured DNA was loaded in duplicate and each well rinsed with 100 µl of 10X SSC. The membrane was then removed from the apparatus and allowed to dry at room temperature followed by baking in a vacuum oven for 2 hours at 80 °C.

Prehybridization was performed for 1 hr at 42 °C in 6X SSPE (1X SSPE is 0.15 M sodium chloride, 0.01 M sodium phosphate monobasic, 0.1 mM EDTA), 5X Denhardts (1X Denhardts is 1% ficoll, 1% polyvinylpyrolidone, 1% bovine serum albumin) solution

and 0.5% SDS. Hybridization was carried out overnight at 42 $^{\circ}$C in the same solution plus $2x10^6$ cpm/ml of either an oligonucleotide containing the normal sequence (#274) or with one containing the A to G transition (#275) (Table 1). After hybridization the membranes were washed twice for 30 min in 6X SSC, 0.5% SDS at room temperature and then autoradiographed with Kodak XOMAT AR film for 2 hours. After this initial exposure the filters were alternately washed at increasing temperatures and autoradiographed until the control dots no longer showed any hybridization to the mutation specific oligonucleotide.

C. Results and Discussion:

The identification of individual PP described here as having residual activity was initially made upon hospitalization at age 54 due to crescendo angina. Examination did not reveal any corneal opacities or angiokeratoma nor was there any history of acroparesthesias or hypohidrosis. A detailed clinical description of this individual has recently been published (103).

Initial studies were carried out in order to determine the amount of α-Gal A activity in various sources from this variant patient with residual activity. As seen in Table 2, the percent of control ranged from 0.81% in granulocytes to 25% in cultured lymphoblasts. Attempts to characterize the physical and kinetic properties of the small amounts of residual enzyme in patient plasma were unsuccessful due to α-N-acetylgalactosaminidase (α-Gal B) activity present in the plasma which also cleaved the artificial substrate. For this reason, enzyme was partially purified (approx. 25 fold) from both residual activity and normal lymphoblasts by affinity chromatography using GalNAc to remove α-Gal B from the affinity column. The partially purified α-Gal A was then used in the characterization studies described below.

Thermostability Studies: Physical characterization studies carried out on partially purified enzyme from the residual activity variant and a normal control individual were performed as described in methods. The results of heat inactivation studies indicated that the stability of the variant enzyme was reduced as compared to the normal enzyme. When incubated at 41 $^{\circ}$C and pH 4.6 the half-life of the variant enzyme was 11 minutes as compared to 33 minutes for the normal enzyme (Figure 2). The instability of the residual activity enzyme was even more pronounced at pH 7.4 where it had a half-life of 8 minutes at 41 $^{\circ}$C as compared to a half-life of 44 minutes for the normal enzyme under these conditions (Figure 2). These findings agreed with the observation that the highest level of residual activity was found in cultured cells (Table 2) where the actively-growing cells were

α-Galactosidase A Activity Levels in Various Sources from a Residual Activity Variant

Enzyme Source	Normal Mean	Variant Activity	% of Normal Activity
Granulocytes (U/mg)	68.2 ± 15.3 (n=21)	0.55	0.81
Lymphocytes (U/mg)	32.6 ± 8.8 (n=20)	0.58	1.78
Lymphoblasts (U/mg)	34.3 ± 9.2 (n=100)	8.60	25.00
Fibroblasts (U/mg)	98.7 ± 27.1 (n=5)	12.00	12.20
Plasma (U/ml)	11.6 ± 4.8 (n=62)	0.67	5.80

Table 2: Determination of α-Gal A activity levels in various sources from normal individuals and from residual activity variant PP. Assays were carried out on plasma and cell extract samples as described in materials and methods. Except for the controls, values are the means of duplicates in a single assay.

Thermal Stability of Partially Purified α-Galactosidase A from a Residual Activity Variant

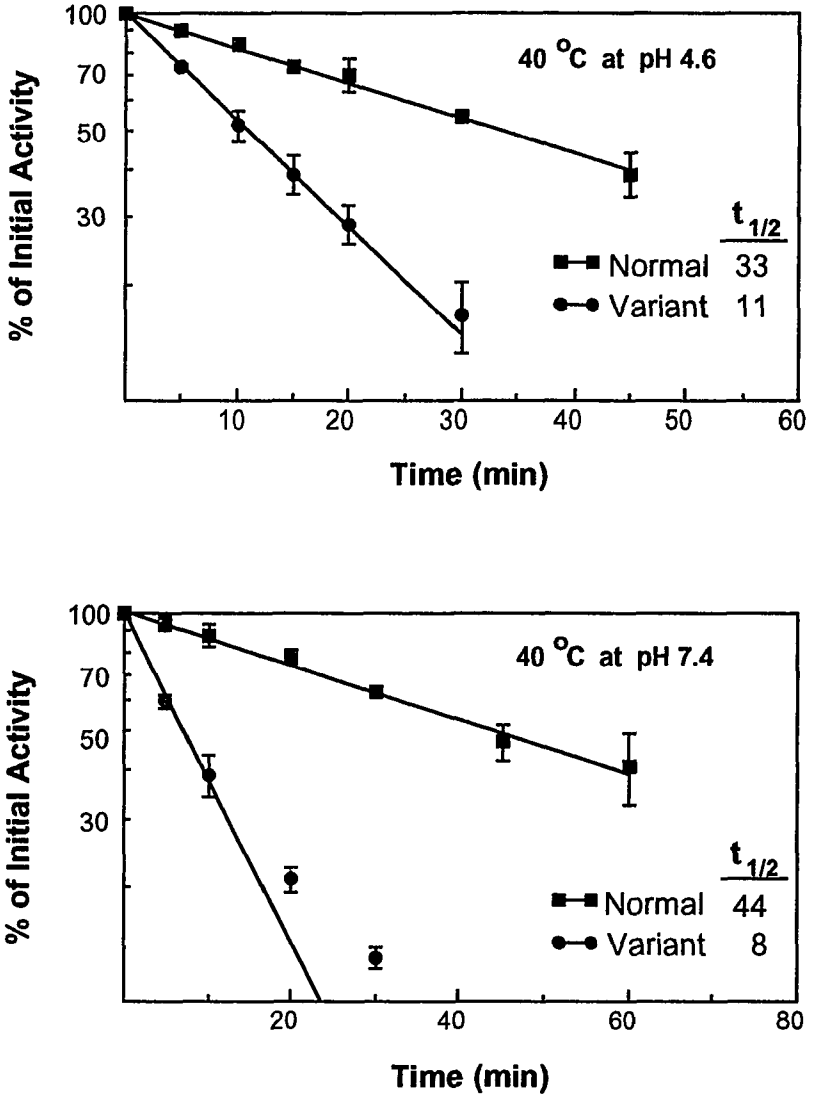

Figure 2: Heat inactivation of partially purified lymphoblast α-Gal A from a normal control or residual activity variant PP. Samples were incubated for the indicated times at 40 °C and either pH 4.6 or 7.4 before being assayed. Graphs show the average of two independent experiments with the error bars representing the standard deviation.

continously synthesizing enzyme up until the time they were harvested and where the enzyme was exposed to a pH at which it was more stable (lysosomal). In contrast, enzyme obtained from plasma would have been exposed to inactivating conditions for a longer period of time.

Kinetic Studies: Kinetic analysis of the residual activity enzyme was next carried out in order to determine if the enzyme's affinity for the substrate or analogs had been altered. The results of these studies using 4MU-α-Gal as the substrate, indicated that the variant enzyme had a slightly higher average K_m than the normal enzyme (4.1 vs 3.0 mM) (Figure 3). This would indicate that the variant enzyme's affinity for the substrate was reduced due to an alteration in the active site of the residual activity enzyme. To further investigate this possibility, studies were carried out using the potent inhibitor D-galacto-deoxynojirimycin. A K_i determination for this inhibitor using either variant or normal enzyme indicated that its effectiveness in inhibiting the variant enzyme was about fourfold less than with normal α-Gal A (Figure 4). The K_i was 70 nM for the normal enzyme and 180 nM for the residual activity enzyme. This finding also indicated that the active site of the variant enzyme has been altered.

Immunoprecipitation Studies: In order to determine if the turnover number (K_{cat}) of the residual activity enzyme was altered, immunoprecipitation experiments were carried out using polyclonal anti-α-Gal A antibodies. During the course of these studies, it was noted that it was never possible to precipitate 100% of the normal activity. Even at saturating antibody concentrations where all of the enzyme protein should be precipitated, only 60 to 70% of the normal activity was found in the pellet (Figure 5A). The remaining activity was not found in the supernatant indicating that inhibition of the normal enzyme, rather than a failure to precipitate normal enzyme protein, was occurring. The presence of soluble, but inhibited, α-Gal A in the supernatant was not possible since a second antibody had been

Kinetic Analysis of Partially Purified Lymphoblast α–Galactosidase A from a Residual Activity Variant

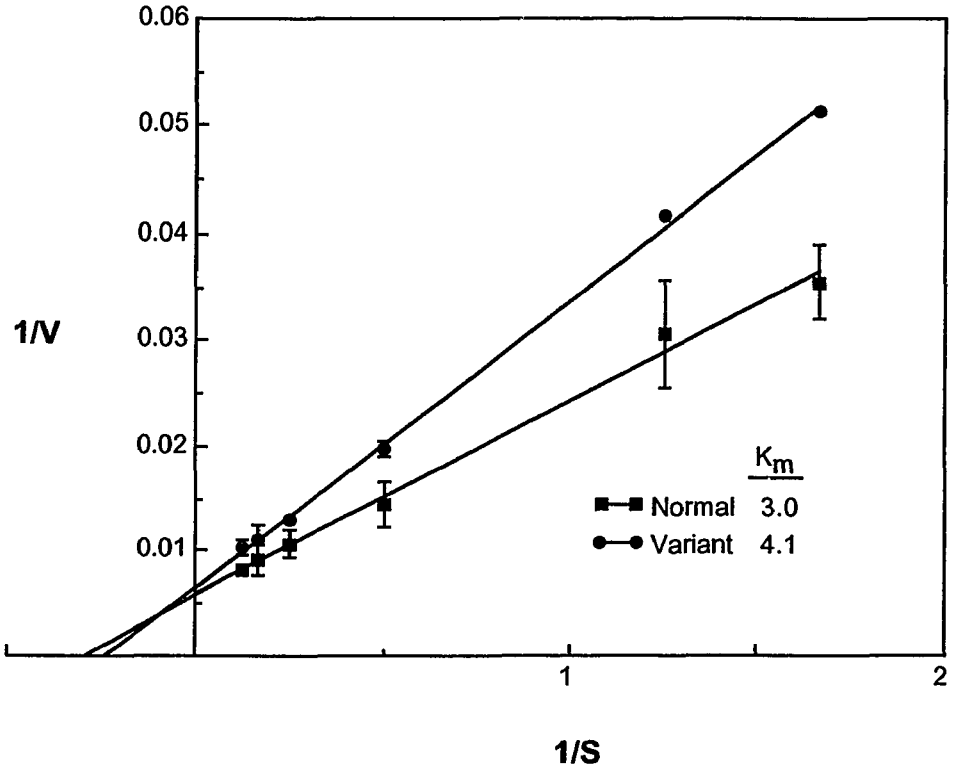

Figure 3: Lineweaver-Burk determination of the K_m of α-Gal A that had been partially purified from the lymphoblasts of a normal control or the residual activity variant. The X-intercept is equal to $-1/K_m$. Graph shows the average of two independent experiments with the error bars representing the standard deviation.

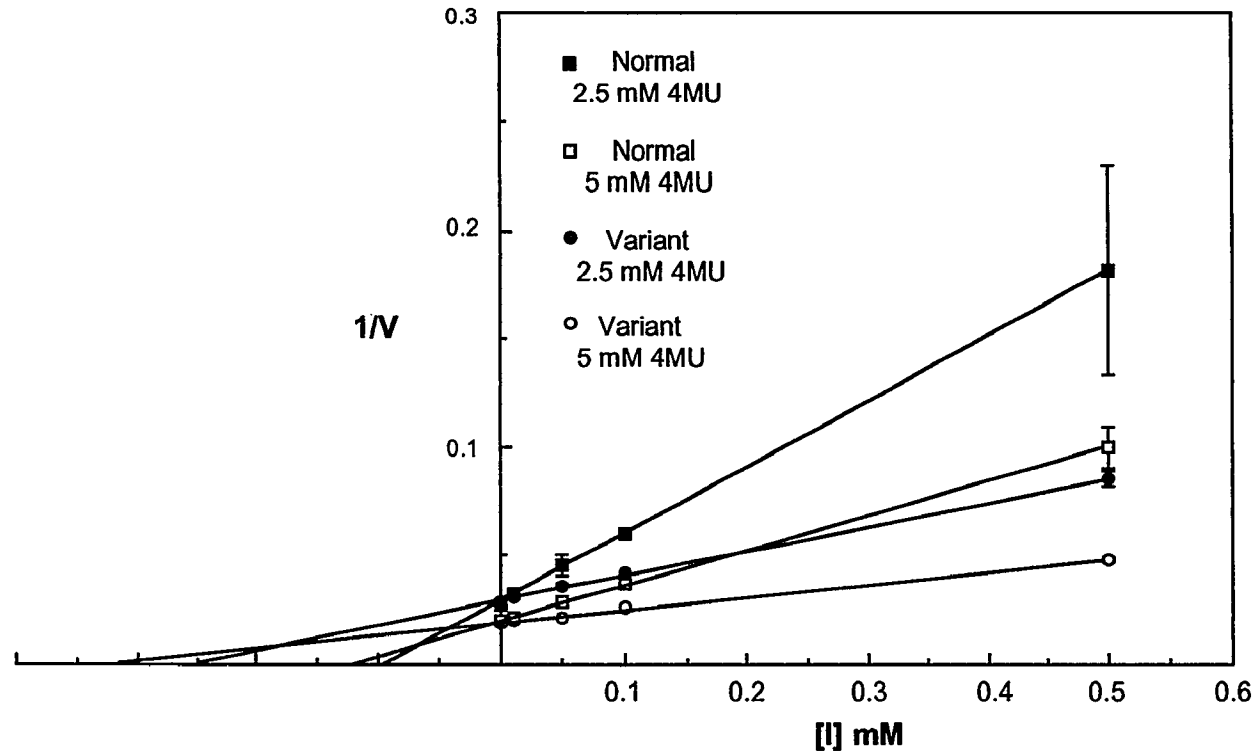

Figure 4: Dixon plot of the inactivation of normal and residual activity α-Gal A by D-galacto-deoxynojirimycin. Inactivation studies were carried out on partially purified enzyme from the lymphoblasts of the residual activity variant (circles) or a normal control (squares) using either 5 mM (open) or 2.5 mM (closed) 4Mu-α-Gal as the substrate. The K_i for the inhibitor is determined by the abscissa value at the intersection of the two lines. These values were determined to be 180 nM for the variant enzyme and 70 nM for the normal control. Graph shows the average of two independent experiments with the error bars representing the standard deviation.

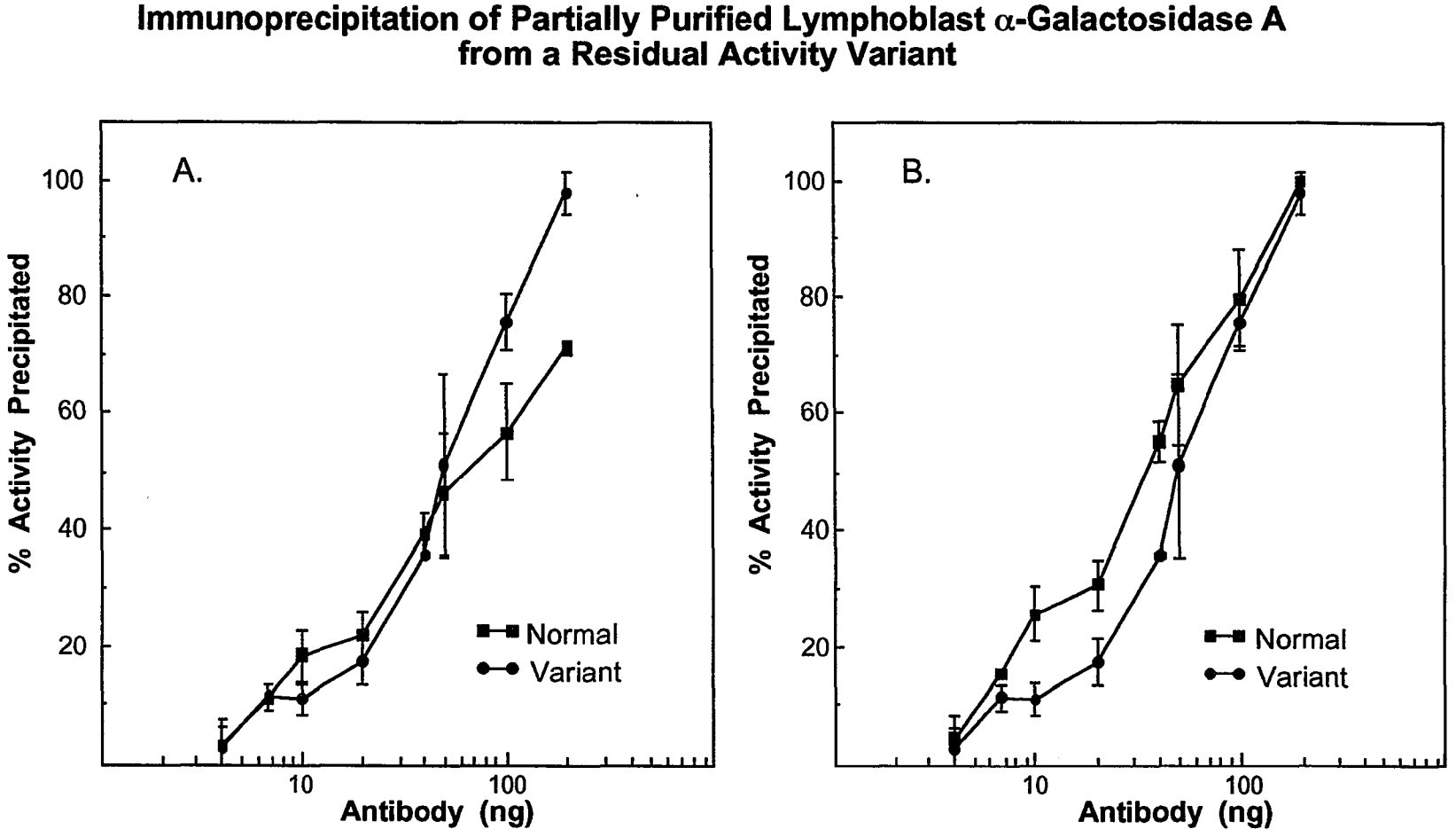

Figure 5: Immunotitration of α-Gal A from a normal control and a residual activity variant. Equal amounts of enzyme activity were precipitated with increasing amounts of anti-α-Gal A polyclonal antibody. Data shown in A has been corrected in B for the inhibition of the normal enzyme by the antibody (see text).

used to precipitate the rabbit anti-α-Gal A antibodies. This finding suggests that some subpopulation of antibody is inhibiting activity by binding to an epitope at or near the active site of the enzyme. In the case of the residual activity enzyme no inhibition of activity was seen, indicating that this epitope had been altered in such way as to render it unrecognizable. This finding supports the kinetic analysis and inhibition studies that have indicated that the active site of the variant enzyme was modified.

The observation that one form of the enzyme was inhibited by the polyclonal antibody while the other was not made the immunoprecipitation data difficult to interpret. For this reason, inhibition of the normal enzyme was corrected by setting the maximum amount of activity precipitated equal to 100% and adjusting the remaining points accordingly (Figure 5B). This adjustment made it clear that precipitation of equal amounts of activity of partially purified variant or normal enzyme required the same amount of antibody. Assuming that the mutation did not alter the immunological titer, this result suggests that the K_{cat} of the two enzymes is the same.

DNA Sequence Analysis: The results of the biochemical characterization of the residual activity enzyme indicated an underlying structural alteration. DNA sequence analysis was carried out in order to determine the molecular nature of this alteration (103). RNA isolated from lymphoblasts from the residual activity variant was reverse transcribed, amplified using PCR and cloned into pGEM-4Z as described in the methods section. Sequencing of the resulting clones revealed the previously identified A to G transition at nucleotide 886 in exon 6 of the α-Gal A cDNA to be the only change from the normal sequence. This mutation, which substituted valine for methionine at residue 296 of the α-Gal A protein (M296V), was confirmed in this thesis research by allele-specific dot blot analysis of PCR-amplified genomic DNA from the residual activity variant (Figure 6). Computer-aided analysis of this region of the α-Gal A protein, using the algorhythym of Chou and Fasman in the GCG computer package, predicted that this mutation would

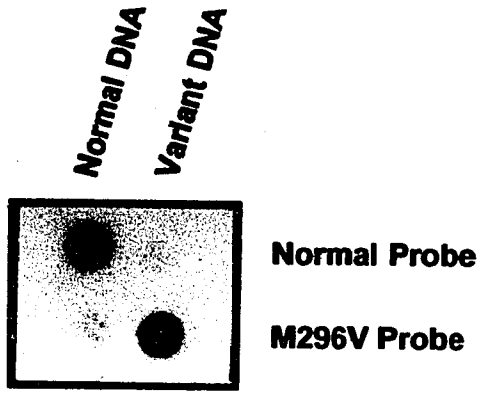

Figure 6: Dot blot analysis of the residual activity allele for the M296V mutation. Gènomic DNA was isolated from the lymphoblasts of the residual activity variant or a normal control, PCR amplified, and hybridized to a probe containing either the normal α-Gal A sequence or one containing the M296V mutation.

change a predicted region of random-coiled structure into a β-pleated-sheet motif (Figure 7). Although the accuracy of the Chou-Fasman prediction has been estimated to be only 45-55% (110,111), the suggestion that the M296V mutation may result in the production of a structurally modified protein is significant. If the computer analysis had failed to predict any structural changes, then the functional changes observed in the residual activity enzyme would be difficult to explain. The suggestion that a structural change does indeed exist indicates that this structural change may be responsible for the altered physical characteristics described above.

Analysis of Additional Cardiac Variants: A residual activity variant with late onset cardiac symptoms caused by a mutation in codon 301 (R301Q) of the α-Gal A protein has recently been described (112). The proximity of this mutation to M296V suggests that these mutations may define a region of the α-Gal A protein that is responsible for their common phenotype. In order to to test this hypothesis, two additional residual activity variants exhibiting cardiac symptoms were analyzed. Screening of these individuals using an oligonucleotide specific to the M296V mutation showed that these individuals lacked this mutation. Exons 5 through 7 of the α-Gal A gene were PCR amplified from genomic DNA isolated from the lymphoblasts from these two individuals. Sequencing of exon 6 was carried out in order to determine if the mutations affecting these individuals would lie within this region. DNA sequence analysis of this region found no changes from the normal α-Gal A sequence. Single-strand conformation polymorphism (SSCP) analysis of the mother of one of the individuals showed a shift in exon 5 indicating that a mutation might be present in this exon (Resnick-Silverman, unpublished). An oligonucleotide specific to a known mutation in exon 5 that resulted in residual activity, due to the presence of a less stable enzyme (Bishop, Eng and Painter, unpublished), was then used to screen amplified DNA from one of the variants and the mother of the other. The results of this were positive indicating that the DNA from both of these variants contained an A to G

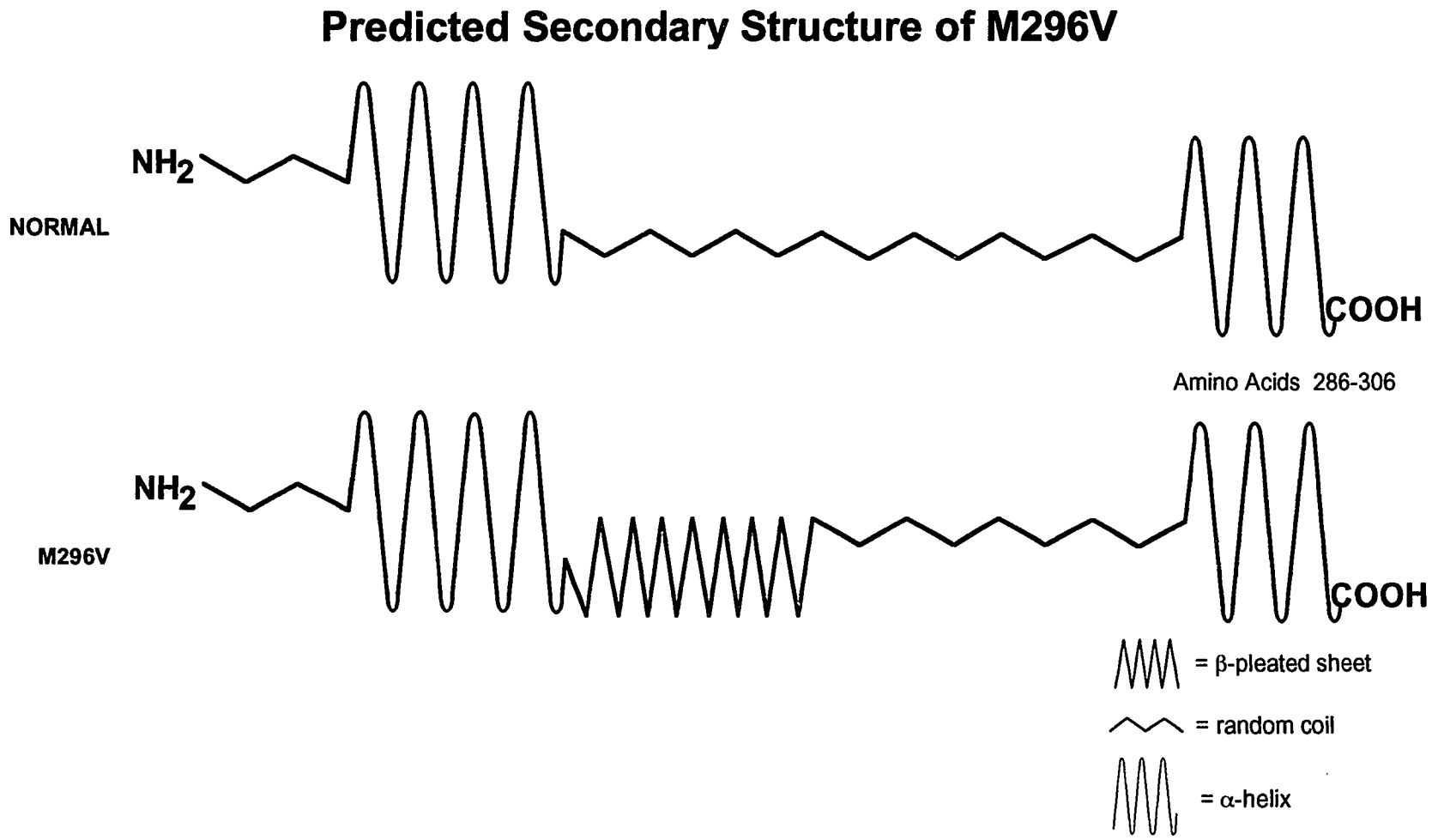

Figure 7: Computer-assisted analysis of the conformational change induced by the G to A transition found in the residual activity allele. The method of Chou and Fasman was used to analyze amino acids 286 to 306 of both the normal and variant enzyme.

transition at nucleotide 644 of the cDNA that resulted in the substitution of serine for asparagine at residue 215 (N215S) of the resulting protein (Figure 8). This mutation was confirmed by sequence analysis (Figure 9). It is interesting to note that this mutation also knocks out a consensus glycosylation sequence as this suggests that this could be the cause of variant activity in these individuals.

The analysis of residual activity variants with a history of cardiac problems has led to the finding of two different mutations with a third mutation reported by Sakuraba, et. al. (112). Each of these mutations leads to the production of a less stable protein. The presence of a less-stable α-Gal A has also been indicated in studies on additional variants whose clinical symptoms were confined to the myocardium (101,102). That residual α-Gal A activity leads to cardiac complications is interesting to note since in classic hemizygotes the kidney is usually the first organ to be effected. The failure to find any significant substrate accumulation in the kidneys of residual activity variants (101,102) may indicate that the kidney is able to remove a certain amount of substrate, possibly by desquamation. In classic hemizygotes, the amount of substrate entering the kidney would be above its clearance threshold thereby leading to accumulation and subsequent failure. In contrast, substrate that enters the tissues of the heart would not be cleared and therefore over time would continue to accumulate leading to cardiac complications. This finding suggests that Fabry's disease should be evaluated in patients with unexplained cardiac symptoms (103).

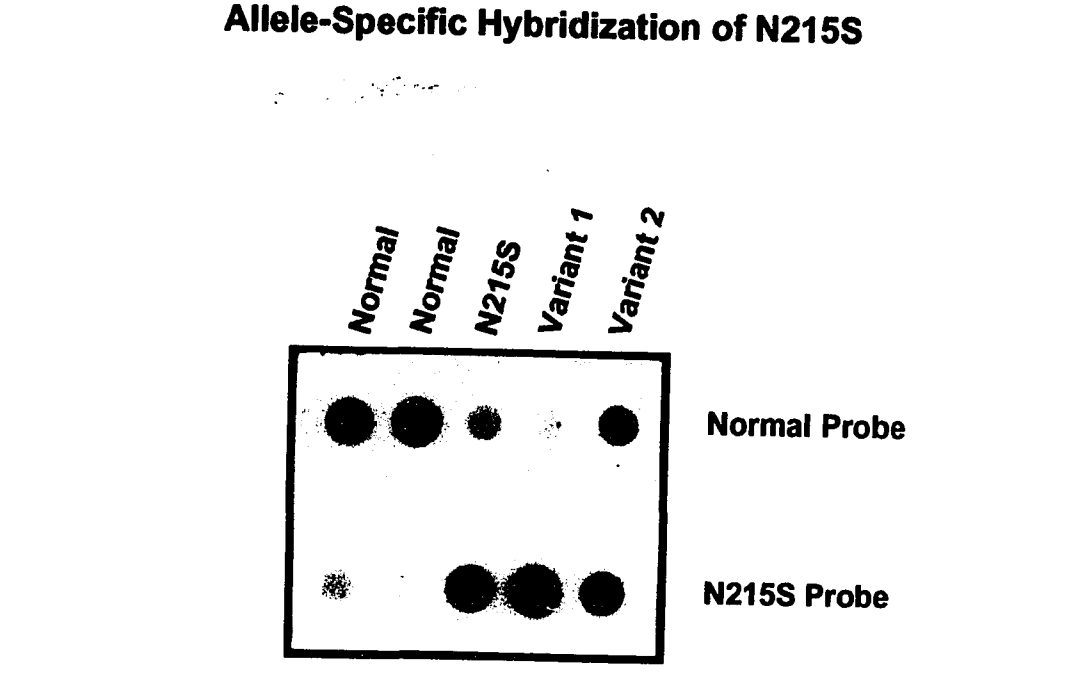

Figure 8: Dot blot analysis of residual activity variants with cardiac symptoms. Genomic DNA was isolated from the lymphoblasts of normal controls, a residual activity variant with a known mutation (N215S), a residual activity variant with cardiac symptoms (Variant 1), or the mother of an additional residual activity variant with cardiac symptoms (Variant 2). DNA was amplified and then hybridized either to a probe containing the normal α-Gal A sequence or one containing the N215S mutation.

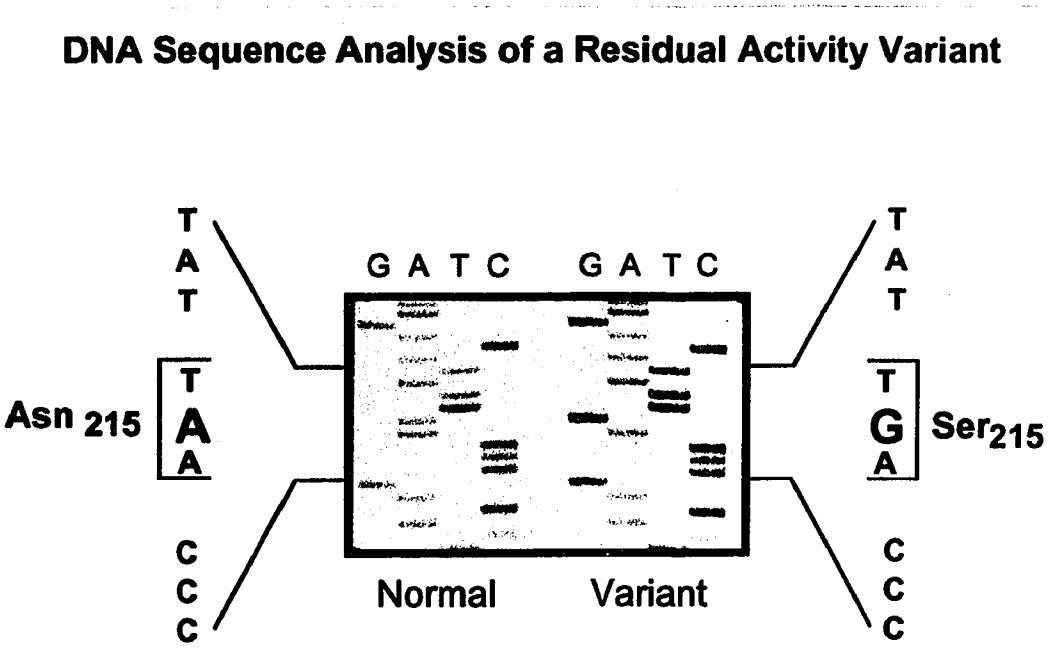

Figure 9: Sequence analysis of a residual activity variant with cardiac symptoms. Genomic DNA was isolated from lymphoblasts, cloned into pGEM-4Z, and sequenced as described in methods.

Chapter 3

Molecular and Biochemical Analysis of the High-Activity Allele

A. **Introduction:**

The incidence of elevated α-Gal A activity levels has been observed in a small percentage of normal individuals (unpublished observation). The possible causes of such elevated activity include increased transcription from the α-Gal A locus, increased stability and/or translation of the α-Gal A message, the presence of an enzyme with increased stability, or the presence of an enzyme with altered kinetic properties. The determination of the causes of elevated activity is of interest as it may provide the means of engineering a form of enzyme that is more suitable for enzyme replacement studies. For this reason, molecular and biochemical studies were directed to determine the cause of increased α-galactosidase A (α-Gal A) activity in an individual whose plasma enzyme level was approximately 3 times above the normal mean. These studies included analyses of thermal stability, K_{cat} and K_m as well as DNA sequence analysis of the high-activity allele. The findings of these studies suggested that, in this case, elevated activity resulted from the increased translation of the high-activity α-Gal A mRNA. *In vitro* transcription and translation of the normal and high-activity alleles was then carried out in order to determine the mechanism by which increased transition leads to increased α-Gal A activity.

B. Materials and Methods:

The methods for α-Gal A assays, partial purification of α-Gal A from lymphoblast extracts, heat inactivation of α-Gal A, K_m determination and immunotitration of α-Gal A are described in chapter 2.

Activity assays of lysosomal enzymes

Enzyme activity assays were carried out at 37 °C on 25 μl of plasma or 10 μl of cell extract using 150 μl of the appropriate 4MU substrate. For β-galactosidase (β-Gal), 1 mM 4MU-β-Gal in citrate-phosphate buffer pH 4.1 was used to assay plasma for 2 hr and cell extracts for 10 min. For β-glucosidase (β-Gluc), the substrate was 16 mM 4MU-β-Gluc in citrate phosphate buffer pH 5.5 and, for β-hexosaminidase (β-Hex), 3 mM 4MU-β-Hex in citrate-phosphate buffer pH 4.4 was used. Assay times for β-Gluc and β-Hex were 10 min for both plasma and cell extracts.

Dot blot quantitation of α-Gal A mRNA levels

Total RNA was isolated by the guanidine isocyanate method (108) and resuspended in diethylpyrocarbonate (DEPC) treated water. Four μg of RNA was heated at 65 °C for 5 min and then rapidly cooled in an ice water bath. The NaCl concentration was adjusted to 0.5 M and the sample was applied in quadruplicate without vacuum to poly U paper (Amersham) that had been equilibrated in 0.5 M NaCl and placed in a dot blot apparatus (Schleicher and Schuell, Keene, NH). When the filter paper had dried, the apparatus was disassembled and the paper was washed twice in 0.5 M NaCl for 5 min, once in 70% ethanol for 2 min, and then air dried. The filter was cut in half, with each half containing the samples in duplicate, and prehybridization was carried out for 5 hr at 42 °C in 5X SSC,

5X Denhardts solution, 50 mM sodium phosphate, pH 6.7, 5% dextran sulphate, 500 mg/ml salmon sperm DNA, and 50% formamide. Hybridization was carried out overnight in the same solution with the addition of 3 x 10^6 cpm/ml of either α-Gal A or actin riboprobe that were made as per manufacturer's instructions (Promega). Following hybridization, the filters were washed at room temperature for 5 min in 4X SSC, 0.1% SDS and then three times at 42 °C for 30 min in 1X SSC, 0.1% SDS and finally for 30 min in 0.1X SSC, 0.1% SDS. The filters were then air dried and autoradiographed using Kodak Xomat AR film.

The relative level of α-Gal A message was determined in the following manner. After autoradiography the dots were cut out and counted in a liquid scintillation counter. The ratio of α-Gal A cpm to actin cpm was determined as a means of equalizing differences in total message amount loaded per sample. For the normal controls, this ratio was averaged and assigned a relative message level of 1.00. The ratio of each sample was then compared to this average in order to determine relative α-Gal A mRNA levels.

Cloning and sequencing of the high-activity allele

Total RNA was isolated from lymphoblasts (108) from the high-activity variant or a normal control. Ten micrograms of RNA was primed with oligo dT and reverse transcribed for 1 hour at 37 °C in a 50 μl reaction containing 50 mM Tris-HCl (pH 8.3), 75 mM KCl, 3 mM $MgCl_2$, 10 mM DTT, 500 μM each dATP, dCTP, dGTP and dTTP, 50 μg/ml oligo dT and 10,000 u/ml reverse transcriptase. The entire α-Gal A cDNA was PCR amplified in two overlapping fragments by using two sets of primers (#210,#273 and #153,#252) and subcloned into pGEM-4Z as described in chapter 2. Double stranded template was isolated from the resulting clones and sequenced by the dideoxy chain termination method using the Sequenase kit (United States Biochemicals, Cleveland, OH) using both universal and α-Gal A specific primers.

In order to analyze 5' flanking sequences, genomic DNA was isolated from the lymphoblasts (109) of the high-activity individual and a normal control. A DNA fragment comprising exon 1, plus 179 bases of 5' flanking sequence, was PCR amplified using oligonucleotide 207 and oligonucleotide 219 (Table 1). Amplified product was digested with *Eco* RI and ligated into pGEM-4Z that had been similarly digested. Positive clones were sequenced as described above. For high-activity individuals identified by plasma screening, the same procedure was followed except that whole blood was used as the source of genomic DNA (113).

Allele-specific hybridization

Genomic DNA was isolated from lymphoblast lines derived from both high-activity individuals and normal controls. A region of exon 1 containing the G to A transition was amplified using oligonucleotide 207 and oligonucleotide 219 as described. One half of the PCR reaction (50 μl) was denatured by adding to 0.4 M NaOH, 25 mM EDTA in a final volume of 400 μl.

A Zeta-Probe nylon membrane was cut to fit a dot blot apparatus (Schleicher and Schuell, Keene, NH) wet in boiling water and then soaked in 2X SSC for 20 min along with a piece of Whatman 3MM filter paper. The filter paper and membrane were assembled into the dot-blot apparatus and each well washed under vacuum with 100 μl of 10X SSC. The denatured DNA was loaded in duplicate and each well rinsed with 100 μl of 10X SSC. The membrane was then removed from the apparatus and allowed to dry at room temperature followed by baking in a vacuum oven for 2 hours at 80 ^{o}C.

Prehybridization was performed for 1 hr at 42 $^{\circ}$C in 6X SSPE, 5X Denhardts solution and 0.5% SDS. Hybridization was carried out overnight at 42 $^{\circ}$C in the same solution plus $2x10^{6}$ cpm/ml of either an oligonucleotide containing the normal sequence (#253) or with one containing the G to A transition (#254) (Chapter 2, Table 1). After

hybridization the membranes were washed twice for 30 min in 6X SSC, 0.5% SDS at room temperature and then autoradiographed using Kodak Xomat AR film for 2 hours. After this initial exposure the filters were alternately washed at increasing temperatures and autoradiographed until the control dots no longer showed any hybridization to the mutation specific oligonucleotide.

In vitro analysis of the high-activity allele

The *Eco* RI insert from pAG18 (31) encoding the mature α-Gal A protein was isolated and cloned into the *Eco* RI site of pGEM-3Z (Figure 10). The resulting plasmid (pG3ZAG18) was cut at unique *Nde* I and *Nco* I sites that are contained within the vector and insert sequences respectively. This resulted in a linearized plasmid from which the T7 promoter sequence as well as the first 46 nucleotides of pAG18 have been removed. PCR was then carried out on genomic DNA from either a normal control or a high-activity individual using primer 272 (Chapter 2, Table 1), containing an *Nde* I site, the T7 promoter sequence plus the 12 bases preceding it in the pGEM-3Z sequence, and 17 bases of α-Gal A sequence beginning at nucleotide -75 from the initiator ATG which has been identified as the transcription start site (114). The antisense primer used (#262) (Chapter 2, Table 1) is complimentary to bases 18 to 35 of pAG18 and includes the *Nco* I site. The product of this reaction was digested with *Nde* I and *Nco* I and ligated into the linearized pG3ZAG18 to recreate the T7 promoter sequence such that transcription from this promoter will initiate at the cap site for α-Gal A. Capped transcripts were produced following the Promega protocol and quantitated by including trace amounts of ^{32}P-labelled CTP in the reaction mix. Equal amounts of transcript from plasmids containing either the normal allele (pG3Z-75) or high-activity allele (pG3ZHA-75) were translated into protein in the presence of ^{35}S methionine using a rabbit reticulocyte lysate as per manufacturers instructions (Promega). Equal volumes of product were analyzed by gel electrophoresis followed by

Construction of Plasmids for the *In Vitro* Production of Normal or High-Activity α-Gal A mRNA

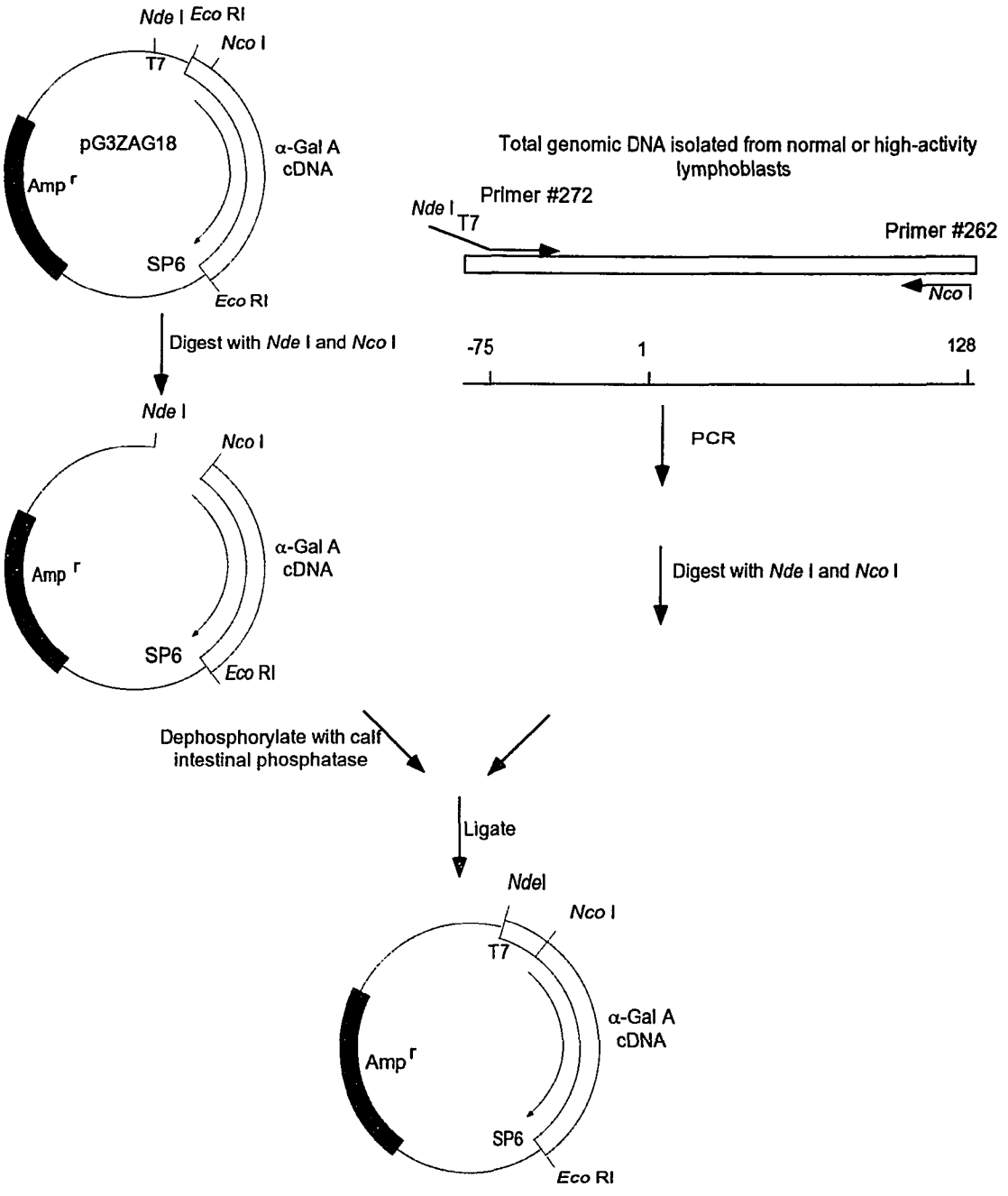

Figure 10: Schematic representation of the production of plasmids used to generate normal or high activity α-Gal A messenger RNA. Plasmids containing either the normal sequence (pGAG3Z) or the G to A transition (pGAGHA3Z) were generated as described in the Methods section.

autoradiography of the labelled proteins in order to determine relative amounts of product formation.

C. Results and Discussion:

A screening of α-Gal A activity in normal individuals identified an individual (EO) whose enzyme activity level was approximately 2.5 times the normal mean. Studies were designed to determine the cause of this increased activity with the hope that an increased understanding of the structure/function relationships present in the normal enzyme would result. The inheritance of the high-activity allele was studied in the proband's family by analysis of α-Gal A activity in plasma. The results of this pedigree analysis are shown in Figure 11. The elevated activity level was clearly seen in the plasma of the high-activity variant (EO) where it was approximately 2.5 times higher than the normal value. The X-linked inheritance of the high-activity allele was demonstrated by the normal activity levels seen in the plasmas of the two sons and the intermediate levels seen in the two daughters plasmas due to lyonization. An interesting observation was that the increased α-Gal A activity level in the plasma was not reflected in cells from either the high-activity variant or his daughters. This indicated that increased secretion of α-Gal A may be occurring from these cell types or, alternatively, that a different cell type is responsible for the increased enzyme activity found in plasma.

Biochemical Studies: In order to characterize the physical properties of the high-activity α-Gal A, enzyme was partially purified from the lymphoblasts of the high-activity variant using affinity chromatography. Studies were then carried out to determine the thermal stability, K_m and K_{cat} of the variant enzyme. None of these studies (Figures 12-14) indicated any difference between the normal and variant enzyme. The immunoprecipitation studies revealed that both the normal and high-activity enzymes were inhibited by the polyclonal antibody (Figure 14A) as described in chapter 2. For this reason, inhibition of both forms of enzyme was corrected by setting the maximum amount of activity precipitated equal to 100% and adjusting the remaining points accordingly

Pedigree Analysis of the High Activity Allele

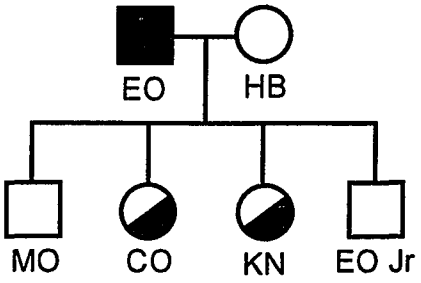

	α-Galactosidase A Activity Level			
	Plasma (U/ml)	**Lymphoblast (U/mg)**	**Granulocyte (U/mg)**	**Lymphocyte (U/mg)**
EO	28.4	43.6		
HB	9.01		11.3	18.0
MO	9.44	21.9	22.4	20.3
CO	20.6	30.0	43.4	19.9
KN	19.0	42.3	35.6	26.9
EO Jr	10.2	51.1	41.4	18.7
Normal	11.6 ± 4.8 (n=62)	34.6 ± 9.2 (n=100)	68.2 ± 15.3 (n=21)	32.6 ± 8.8 (n=20)

Figure 11: Pedigree analysis of the high activity allele demonstrating the X-linked mode of inheritance. Except for the controls, values are the means of duplicates in a single assay.

Thermal Stability of Purified α-Galactosidase A from a High Activity Variant

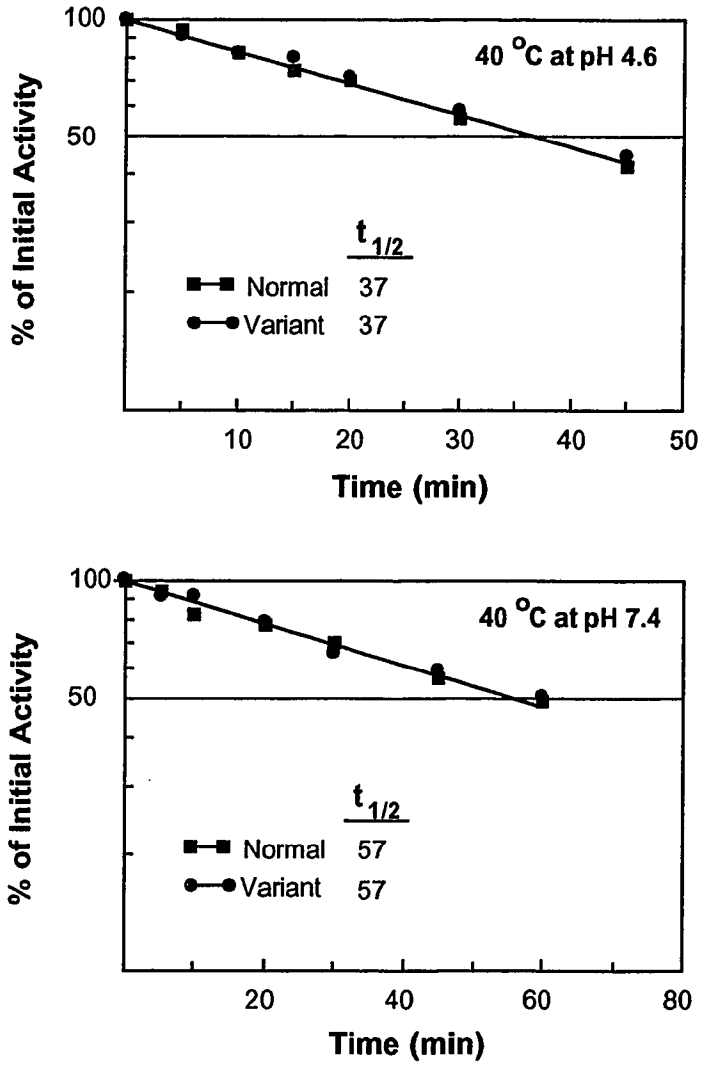

Figure 12: Heat inactivation of partially purified lymphoblast α-Gal A from a normal control or a high activity variant (EO). Samples were incubated for the indicated times at 40 °C and either pH 4.6 or 7.4 before being assayed. Graphs represent the results of a single experiment.

Kinetic Analysis of Purified Lymphoblast α-Galactosidase A from a High-Activity Variant

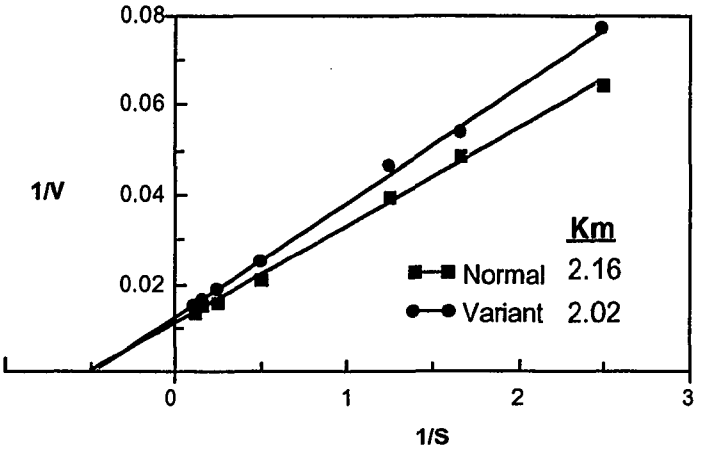

Figure 13: Lineweaver-Burk determination of the K_m of α-Gal A purified from the lymphoblasts of a normal control or the high activity variant. The X-intercept is equal to $-1/K_m$. Graph is the result of a single K_m determination.

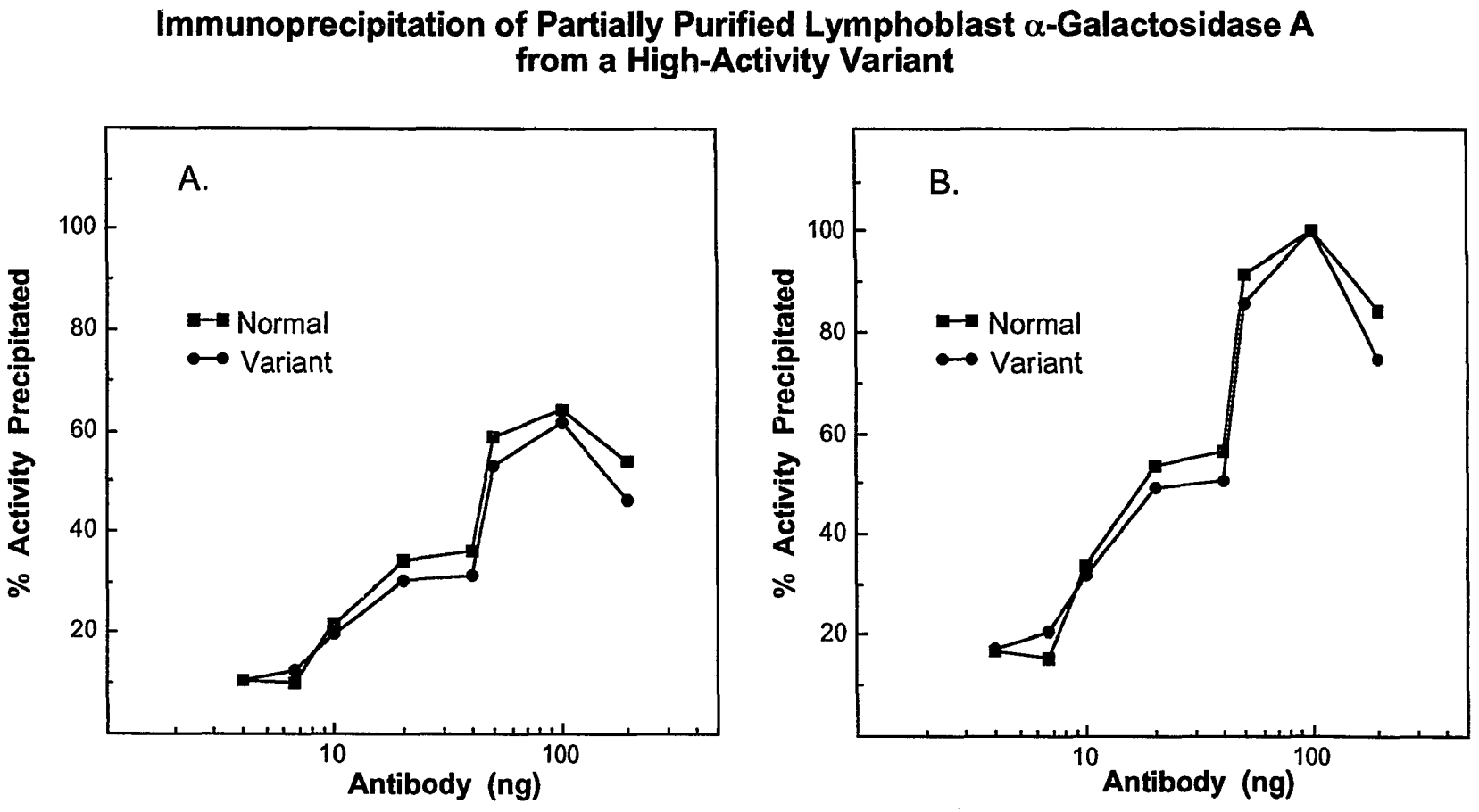

Figure 14: Immunotitration of α-Gal A from a normal control and a high-activity variant. Equal amounts of enzyme activity were precipitated with increasing amounts of anti-α-Gal A polyclonal antibody. Data shown in A has been corrected in B due to inhibition of both the normal and high-activity enzyme by the antibody (see text). Graphs represent the results of a single experiment.

(Figure 14B). The finding that the K_{cat} of the variant enzyme was normal indicated that the increased α-Gal A activity levels must be resulting from an increased amount of enzyme protein. Since the stability of the variant enzyme was normal, an increase in enzyme protein levels could be caused by either increased transcription of the α-Gal A gene or the presence of a more stable or more efficiently translated α-Gal A messenger RNA.

RNA Dot Blot Analysis: An increase in either transcription of the α-Gal A gene or the stability of its message should result in an increased level of α-Gal A mRNA. Although cellular α-Gal A activity levels were normal in the high-activity individual, it was possible that a higher cellular message concentration would result in secretion rather than accumulation. Therefore, dot blot analysis was carried out in order to determine if α-Gal A mRNA levels were elevated in the high-activity variant. Total RNA was isolated from the lymphoblasts of the high-activity variant and two normal controls and used to determine α-Gal A mRNA levels relative to actin mRNA as described in the methods section. The combined results of four such experiments are shown in Table 3. α-Gal A mRNA levels were not significantly elevated in the high-activity variant's lymphoblasts.

DNA Sequence Analysis: Since all of the physical properties of the variant enzyme were normal, it was unlikely that the causative mutation was in the coding sequence. This was shown to be correct as the sequence of the entire α-Gal A coding region was identical to the normal sequence. In order to further examine upstream noncoding sequences, a DNA fragment containing exon 1 plus 179 nucleotides of upstream 5' flanking sequence, was amplified from genomic DNA isolated from lymphoblasts from the high-activity variant (EO). This fragment was cloned into pGEM-4Z and sequenced. The analysis revealed a G to A transition 30 nucleotides 5' of the first translated codon of the α-Gal A cDNA (Figure 15). This mutation also eliminated a *Sac* II restriction site. This mutation, located in the 5' noncoding sequence of the α-Gal A mRNA, could result in elevated

Relative α-Galactosidase A mRNA Level						
Sample	Assay 1	Assay 2	Assay 3	Assay 4	Avg	SD
Variant	0.97	1.52	1.34	1.16	1.25	0.21
Normal 1	1.16	1.11	0.85	0.85	0.99	0.14
Normal 2	0.83	0.90	1.16	1.15	1.01	0.15

Table 3: Dot blot analysis of the relative levels of α-Gal A messenger RNA in lymphoblast extracts from a high activity variant (EO) or normal controls. Total RNA was dot blotted as described in methods and the results of four such trials are shown above along with average values (Avg) and standard deviations (SD).

DNA Sequence Analysis of the High-Activity Allele

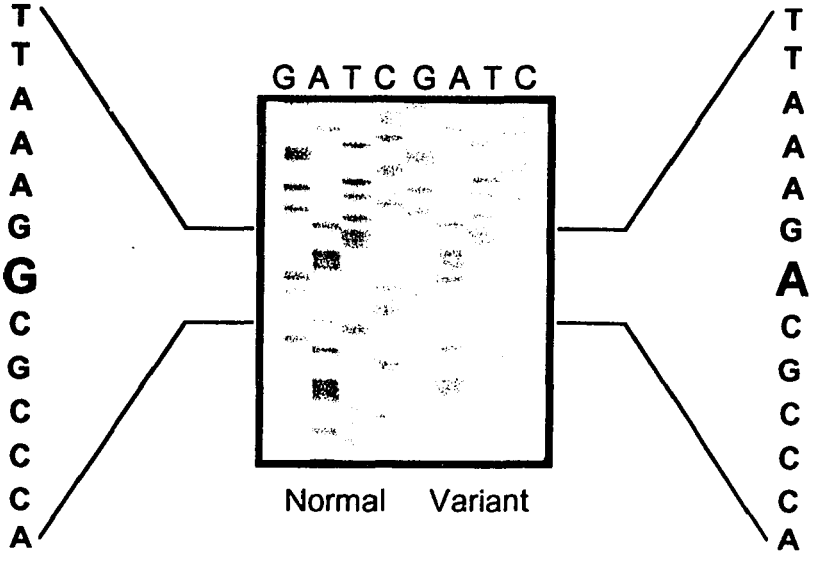

Figure 15: Sequence analysis of the high-activity allele. Genomic DNA was isolated from lymphoblasts, cloned into pGEM-4Z, and sequenced as described in methods.

activity levels by increasing the translational efficiency of the message by an unknown mechanism.

Analysis of Additional High-activity Variants: If this mutation was the cause of increased α-Gal A activity then it should be inherited in an X-linked manner and might also be found in other, unrelated high-activity variants. To determine the frequency of the high-activity mutation in the general population, 400 random blood samples were obtained from the clinical hematology department of the Mount Sinai Medical Center and assayed for plasma α-Gal A activity. Genomic DNA was isolated from samples that had activity levels greater than twice the normal value and the region containing the G to A transition was PCR amplified. The presence of the mutation was then detected by digestion with *Sac* II. Of the 400 samples assayed, 29 were found to have activity levels that were ≥ 2 times the normal mean (Figure 16) and of these, 2 tested positive for the G to A transition (HF, HS). An additional individual (ES), that had been identified as being a high-activity variant during an earlier sampling of normal individuals, also tested positive for this mutation. Since the identification of the G to A transition was based on the failure of *Sac* II to digest the amplified DNA, the possibility existed that identification of the mutation in these individuals resulted from inefficient enzyme digestion rather than the presence of the actual mutation. In order to rule out this possibility, allele-specific hybridization was carried out on DNA from these 3 individuals (Figure 17). Allele-specific hybridization was also carried out on DNA from the original high-activity family (Figure 11) in order to confirm the X-linked inheritance of the mutation (Figure 17). This mode of inheritance is shown by the fact that the sons of high-activity variant EO carry only the normal allele while the daughters are heterozygous for the mutation.

Consistent with the finding of this mutation in the 5' noncoding sequence of α-Gal A, there was no evidence that increased α-Gal A activity was the result of a more generalized lysosomal trafficking disorder. The activity levels of several different

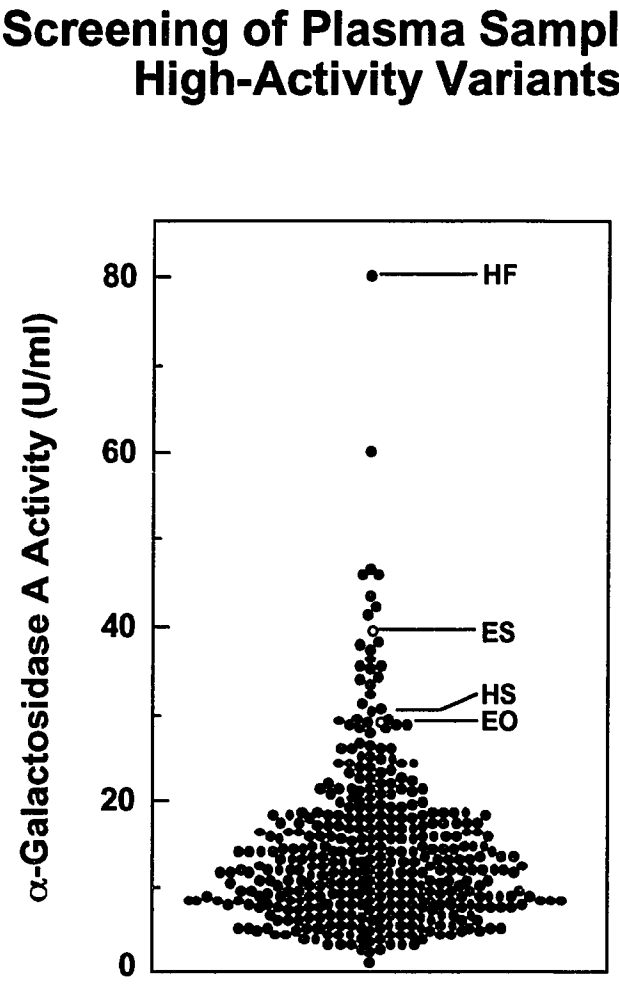

Figure 16: Analysis of the results of the determination of α-Gal A activity in 400 randomly obtained plasma samples. The activity levels of two previously identified high-activity variants are also shown with open circles (∘).

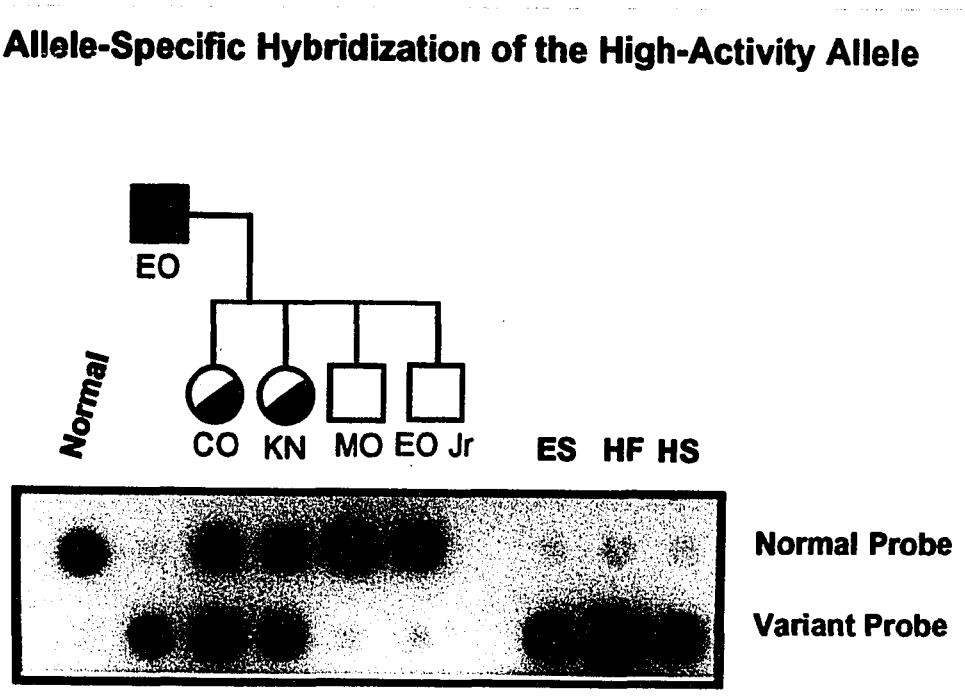

Figure 17: Dot blot analysis of the high-activity allele. Genomic DNA was isolated from the lymphoblasts of a normal control, members of the high-activity pedigree, and high-activity variant ES. DNA was also isolated from whole blood from two individuals identified as having high-activity during a screening of 400 randomly obtained blood samples (HF and HS). The DNA was then hybridized to either an oligonucleotide containing the normal α-Gal A sequence or one containing the G to A transition.

lysosomal enzymes were determined in a blood sample taken from high-activity variant ES. The results of these assays, as shown in Table 4, indicated that the increased enzyme activity was specific to α-Gal A and therefore is not a generalized phenomenon.

The finding that 29 of the randomly assayed samples had elevated activity levels while only 2 of them had the -30 mutation is interesting to note. This obviously means that there is more than one cause of elevated α-Gal A activity. It is possible that, since these samples were obtained from individuals that had been admitted to the hospital for one reason or another, the increased α-Gal A activity level is in someway related to their existing disease state. Alternatively, since the enzyme from these additional high-activity variants was not characterized, it is quite possible that changes in the enzyme's stability, substrate affinity and/or specific activity may be the cause of the increased α-Gal A activity. Another interesting possibility is that increased transcription of the α-Gal A gene or increased translation of the α-Gal A mRNA is occurring in some of these individuals due to a different mutation in the 5' flanking and 5' exonic noncoding sequences. In order to examine this possibility, 254 nucleotides of 5' flanking region, including the noncoding region of exon 1, was sequenced from 5 of these individuals. No changes from the normal sequence were found (data not shown) indicating that increases in the level of translation or transcription is not responsible for the variant activity exhibited by these individuals.

***In Vitro* Studies of Translation Efficiency:** The possibility that the -30 G to A transition causes increased translation of the α-Gal A mRNA was next examined. Computer-aided determination of secondary structure in the 5' leader sequence of the α-Gal A mRNA was carried out using the RNA fold program of M. Zucker (115). A comparison of the secondary structures determined for the 5' leader sequences of both the normal and high-activity mRNAs is shown in Figure 18. As illustrated in the figure, the G to A transition destabilizes a moderately stable (ΔG=-15.2 kcal) stem-loop structure contained in the 5' leader sequence of the normal message resulting in a predicted structure with a ΔG of

LEVELS OF SELECTED LYSOSOMAL ENZYMES

	Plasma		Granulocytes		Lymphocytes	
Enzyme	Variant (U/ml)	Normal (U/ml)	Variant (U/mg)	Normal (U/mg)	Variant (U/mg)	Normal (U/mg)
α-Gal A	39.5	11.6 ± 4.6	111.0	84.5 ± 22.4	52.5	40.6 ± 8.3
β-Hex	713.0	620.0 ± 184.0	1920.0	1840.0 ± 240.0	1100.0	1310.0 ± 250.0
β-Gal	20.3	31.0 ± 10.2	308.0	237.0 ± 43.6	195.0	239.0 ± 38.0
β-Gluc	56.1	87.0 ± 53.2	263.0	424.0 ± 116.0	480.0	447.0 ± 101.0
α-Man	35.9	28.4 ± 8.1	679.0	904.0 ± 143.0	202.0	158.0 ± 58.2

Table 4: Enzyme activity levels were determined in both plasma and cell extracts from ten normal individuals and high activity variant (ES). Enzyme levels were determined for α-galactosidase A (α-Gal A), β-Hexosaminidase (β-Hex), β-galactosidase (β-Gal), β-glucosidase (β-Gluc) and α-mannosidase (α-Man). Normal values represent the average of the ten control individuals.

Predicted Secondary Structure of the 5' Noncoding Regions of Normal and High Activity α-Galactosidase A Messenger RNAs

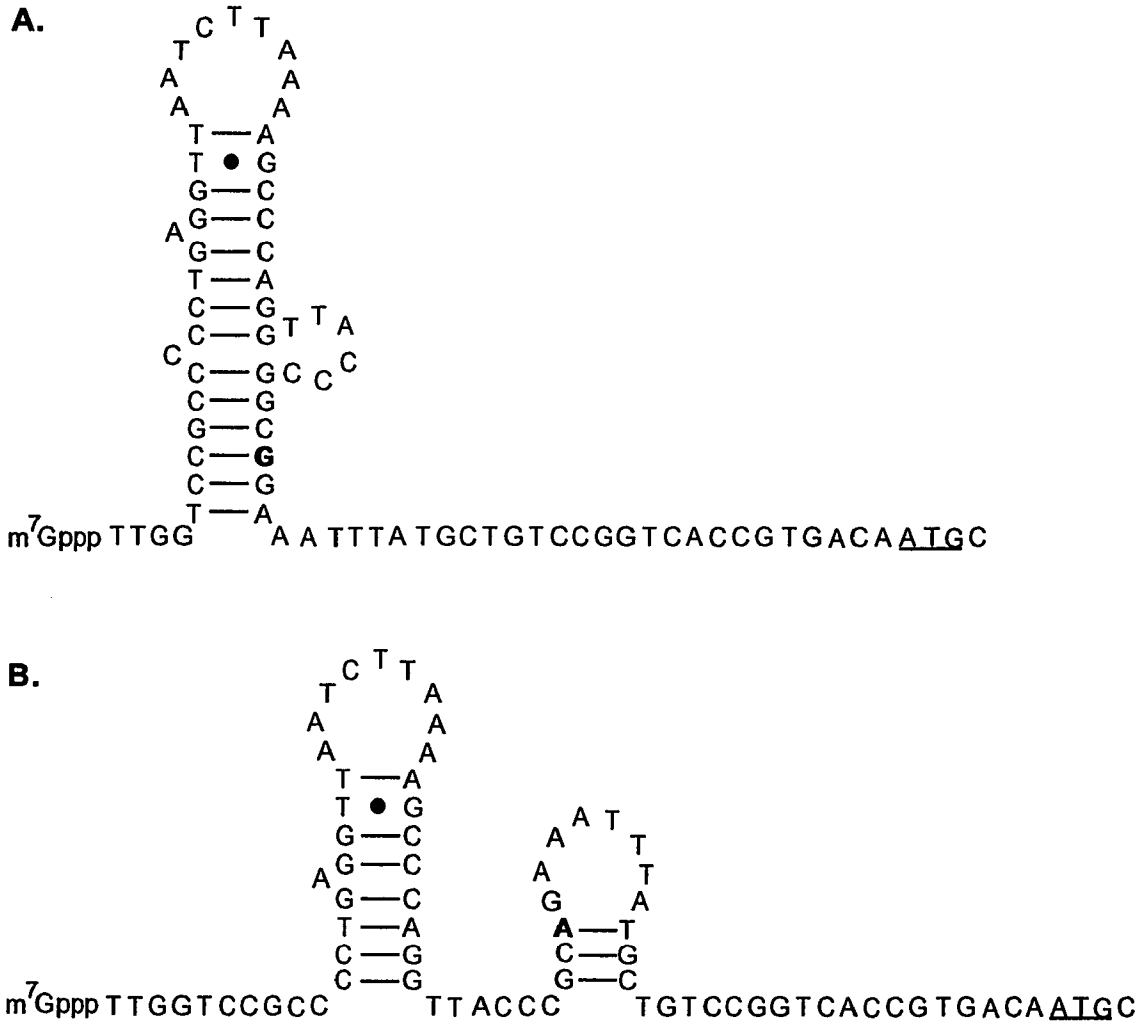

Figure 18: Computer assisted analysis of the 5' leader sequence of the α-Gal A mRNA predicts the presence of a stem- loop structure with a ΔG value of -15.2 located 5 bases downstream from the cap site (A). The G to A transition that is found at nucleotide -30 of the high activity allele destabilizes this structure thereby favoring the formation of the secondary structure shown in B (ΔG= -9.1). The nucleotides involved in this transition are shown in bold and the initiator ATG is underlined.

-9.1 kcal. Although the normal structure is not of sufficient stability to inhibit translation on its own (42-46), it may interact with some unidentified inhibitory protein factor in a fashion similar to the mRNA for ferritin (74). The secondary structure change induced by the high-activity mutation may reduce or completely inhibit the binding of this factor thereby leading to increased translation. Alternatively, this mutation may increase translation by making the 5' end of the message more accessible to the 40S ribosomal subunit. This type of mechanism would be in agreement with studies that have determined that moderately stable stem-loop structures located within 12 bases of the cap site lead to reduced translational efficiency (42).

In order to further examine these possibilities, the high-activity and normal cDNAs were cloned into pGEM-3Z in order to generate *in vitro* transcripts for subsequent *in vitro* translation studies. A major disadvantage in examining translational effects using messages transcribed *in vitro* is that these messages usually contain a certain number of nucleotides derived from the vector. These extra bases also tend to be very G-C rich and therefore significantly change the secondary structure of the message being studied. In order to avoid such effects the cloning scheme illustrated in Figure 10 was devised. The construction of these plasmids, as described in the methods section, resulted in only the addition of a G residue to the 5' end of the α-Gal A message upon *in vitro* transcription from the T7 promoter. The presence of this G residue was necessary in order to permit addition of a 5' cap to the message during transcription. *In vitro* translation studies in rabbit reticulocyte lysates using equal amounts of either normal or high-activity messages yielded the same amount of α-Gal A protein (Figure 19). Great care was taken during the course of this experiment to ensure that the results were not influenced by either the amount of RNA used in the translation reaction or by RNase contamination. First, the *in vitro* transcription reactions were carried out on equal amounts of either normal or high-activity template in the presence of trace amounts of ^{32}P-labelled CTP. Then, each of the messages was diluted 1:10 in 1 mg/ml tRNA and 5 μl was counted in a liquid scintillation counter.

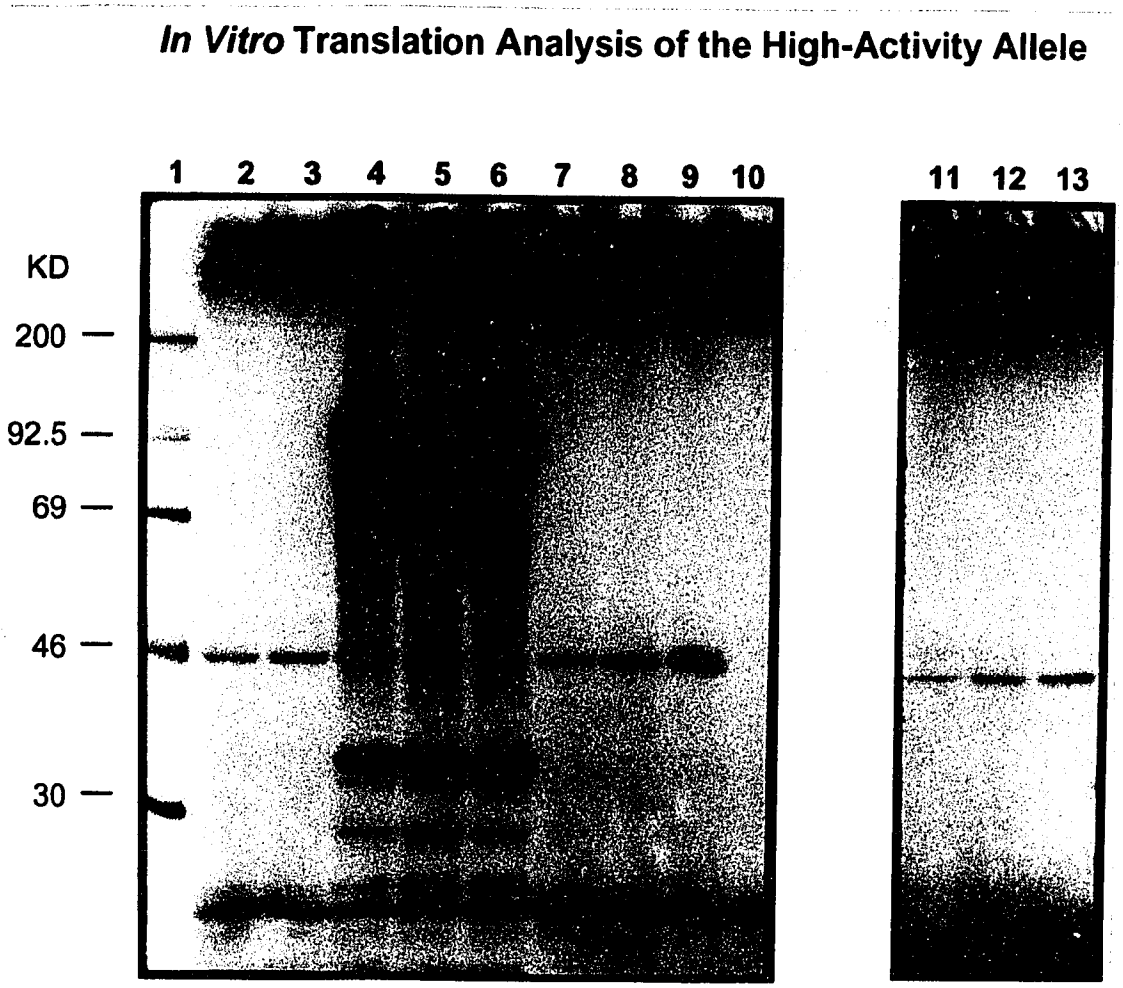

Figure 19: *In vitro* translation analysis of the high-activity allele. Translation was carried out on transcripts prepared *in vitro* from plasmids containing either the normal α-Gal A sequence or the G to A transition. Normal or high-activity transcripts were also mixed with brome mosaic virus (BMV) RNA and then translated as a control for RNase contamination. Lane 1: molecular weight standards. Lane 2: normal transcript (4 ml). Lane 3: high-activity transcript (4 ml). Lane 4: Normal transcript (4ml) +BMV RNA (2ml). Lane 5: high-activity transcript (4 ml) + BMV RNA (2 ml). Lane 6: BMV RNA (2ml) Lanes 7-9: 2, 4, or 8 ml of normal transcript. Lane 10: no RNA. Lanes 11-13: same samples as lanes 7, 8, 9, run on a different gel.

The same number of CPM of each message was used for the *in vitro* translation reactions thereby ensuring that the same amount of each message was used. The linear response of protein produced to input RNA was demonstrated by using increasing amounts of the normal message in the translation mix (Figure 19, lanes 11-13). Finally, in order to rule out the presence of RNase contamination in one of the samples that could lead to degradation during the translation reaction, each of the two messages was mixed with control RNA and translated (Figure 19, lanes 4-6).

The findings of the *in vitro* translation analysis leave open the possibility that the differential translation of the normal and high-activity α-Gal A messages is a specific event in some as yet unidentified cell type. This would explain the normal α-Gal A activity levels observed in the granulocytes, lymphocytes and lymphoblasts isolated from the high-activity variant. Some of the excess α-Gal A from the overproducing cells is presumably secreted thereby leading to the increased amount of plasma activity seen in the variant individuals.

A range of α-Gal A activity has been observed in various cell types. These activities range from 32.6 U/mg in lymphocytes to 98.7 U/mg in fibroblasts. The results presented here indicate that these differences could be due to differences in α-Gal A translation levels in different cell types. This could be explained by the differential expression of an α-Gal A specific translation factor but this would seem an unlikely mechanism for a housekeeping gene. It is more likely that differential translation occurs due to the normal competition between α-Gal A messenger RNA and other cellular messengers for a limiting amount of translation initiation factors. The constituitive levels of these factors vary from cell type to cell type thereby determining the degree of competition that exists. In cells where initiation factors are relatively abundant, all messages would be translated at high levels. When initiation factors are limiting, however, the amount of a particular protein that is produced would depend on how well its corresponding message is able to compete for the limiting initiation factors. One of the main determinants of a messenger RNA's "competetiveness" is the secondary structure found in its 5' noncoding

sequence. Studies have shown that the less secondary structure present in the leader sequence of the mRNA, the more competitive the message is with respect to translation (41,43,44,116). This observation may provide the basis for explaining the differential translation of the normal and high-activity α-Gal A messages. Under normal conditions α-Gal A is translated at a certain basal level based on its competitiveness as compared to the rest of the messages present within the cell. This level would be different for different cell types depending on the level of initiation factors present within the cell. Certain cell types would tend to be more competitive and therefore would be more sensitive to changes in the 5' secondary structure of a particular mRNA. The secondary structure change induced by the high-activity mutation may make the variant message more competitive in these cell types therefore leading to the increased production of α-Gal A protein. This phenomena would not be expected to be mimicked in an *in vitro* system where no competition is taking place.

Suggested Additional Studies: The determination of the cause of the increased translational efficiency of the high-activity mRNA poses an interesting problem that may be analyzed by several different methods. The suggestion that the increased translation results from the interaction of some cell-specific factor with the α-Gal A message could be addressed by adding nuclease-treated extracts from different cell types (i.e. fibroblasts, endothelial cells) to the *in vitro* translation mix. If such a protein factor exists, addition of the cell extract containing the factor should lead to differential translation of the high-activity and normal messages *in vitro*. The cell extracts could also be used in gel-shift assays in order to determine if a tissue-specific protein factor is present that binds preferentially to the mutant or normal form of the α-Gal A message.

In vivo studies could also be designed to study this phenomena. Transfection of different cell types could be performed using constructs consisting of either the normal or high-activity 5' noncoding sequence fused to a reporter gene (i.e. chloramphenicol

acetyltransferase). Expression of the reporter gene could then be normalized by cotransfecting with a control plasmid (i.e. β-galactosidase) in order to determine if a cell-specific increase in translation was taking place. If this method identified a cell-type in which increased α-Gal A activity was occurring, one could then examine whether a cell-specific protein factor or local concentrations of initiation factors was responsible for the increase in translation. The mechanism may be based on the proximity of the stem-loop structure shown in figure 18 to the cap site or a sequence-specific interaction between the 5' noncoding region and a sequence contained within the α-Gal A cDNA. Alternatively, some form of interaction may exist between the 5' noncoding region and the poly(A) tail. Sequence-specific interactions of this type could theoretically be weakened by the G to A transition found in the high-activity allele thereby leading to increased translational efficiency.

If the reduced secondary structure of the high-activity mRNA leads to increased translation by increasing the message's ability to compete for limiting amounts of initiation factors, then a further reduction in secondary structure should lead to an even higher level of translation. Experiments of this type could be carried out using site-directed mutagenesis techniques followed by translation either *in vitro* or *in vivo*. Mutations of other nucleotides in the 5' noncoding sequence may also provide information about sequence-sequence interactions that are important for translation. The question of whether or not the 3' poly(A) tail plays a role in translation could be addressed by modifying its length through the use of synthetic linkers. The constructs used in the translation experiments described here contained a poly(A) tail of 14 residues at their 3' end. A longer poly(A) tract may be necessary before any effect on translation is apparent.

An alternative method for identifying the source of increased α-Gal A activity is the use of transgenic mice. Standard methods could be used to create mice that contain either the normal or high-activity allele in single copy number. Although this approach is time-

consuming and not without problems, it could provide detailed information on α-Gal A translation in all tissues.

Concluding Remarks:

The studies described here have been designed to determine the cause of variant α-Gal A activity. In order to accomplish this, biochemical and molecular studies were carried out on enzyme from a residual activity variant as well as an individual with elevated enzyme activity. In the case of the former, the variant activity was shown to be the result of the presence of a less stable enzyme with reduced affinity for the substrate. Molecular analysis revealed an A to G transition at nucleotide 886 of the cDNA to be the underlying mutation.

The analysis of the high-activity variant proved to be more challenging. Characterization of the α-Gal A enzyme from this individual indicated that the enzyme was normal. The increased activity present was determined to be caused by an increased amount of enzyme protein based on K_{cat} determination. Dot blot analysis of α-Gal A message levels determined that this increase was not due to either an increase in transcription from the α-Gal A locus or the presence of a more stable message. Sequence analysis of the high-activity allele revealed a G to A transition in the 5' noncoding sequence of the α-Gal A message. This mutation presumably results in increased protein levels by increasing the translational efficiency of the α-Gal A message by changing the secondary structure of its 5' noncoding sequence. Attempts to demonstrate this *in vitro* were unsuccessful indicating that the effect of this mutation may only be seen in certain cell types. This conclusion is based on the theory that the level of competition between messages varies from cell to cell and that the competitiveness of a particular message is influenced by the secondary structure of its leader sequence.

References

1. Brady RO, Gal AE, Bradley RM, Martensson E, Warshaw AL and Laster L: Enzymatic defect in Fabry's Disease: Ceramide trihexosidase deficiency. *New England Journal of Medicine* 276:1163,1967.

2. Anderson W: A case of angiokeratoma. *British Journal of Dermatology* 10:113,1898.

3. Fabry J: Ein beitrag zur kenntras der purpura haemorrhagica nodularis (Purpura papulosa hemorrhagica Hebrae). *Archiv füer Dermatologie und Syphilis* 43:187,1898.

4. Steiner L and Voerner H: Angiomatosis milaris: eine ideiopathische gefasserkrankung. *Deutsches Archiv für Klinische Medizin* 96:105,1909.

5. Gunther H: Anhidrosis und diabetes insipidus. *Zeitschrift für Klinische Medizin* 78:53,1913.

6. Weicksel J: Angiomatosis, bzw. angiokeratosis universalis (eine sehr seltent haut- und gafasskrankheit). *Deutsche Medizinishe Wochenschrift* 51:898,1925.

7. Pompen A, Ruiter M and Wyers J: Angiokeratoma corporis diffusum (universale) Fabry, as a sign of an unknown internal disease: two autopsy reports. *Acta Medica Scandinavica* 128:234,1947.

8. Sweely C and Klionsky B: Fabry's disease: classification as a sphingolipidosis and partial characterization of a novel glycolipid. *Journal of Biological Chemistry* 238:3148,1963.

9. Opitz J, Stiles F and Wise D: The genetics of angiokeratoma corporis diffusum (Fabry's disease) and its linkage to the Xg locus. *American Journal of Human Genetics* 17:325,1965.

10. Kint J: Fabry's disease: alpha-galactosidase deficiency. *Science* 167:1268,1970.

11. Dean K, Sung S and Sweely C: The identification of α-galactosidase from human liver as an α-N-acetylgalactosaminidase. *Biochemical and Biophysical Research Communications* 77:1411,1977.

12. Schram A, Hamers M and Tager J: The identity of α-galactosidase B from human liver. *Biochemica et Biophysica Acta* 482:138,1977.

13. Beutler E and Kuhl W: Purification and properties of human α-galactosidases. *Journal of Biological Chemistry* 247:7195,1972.

14. Rietra PJ, Van den Bergh FA and Tager JM: Properties of residual α-galactosidase activity in the tissues of a Fabry hemizygote. *Clinica Chimica Acta* 62:401,1975.

15. Beutler E and Kuhl W: Biochemical and electrophoretic studies of α-galactosidase in normal man, in patients with Fabry's disease, and in equidae. *American Journal of Human Genetics* 24:237,1972.

16. Kusiak J, Quirk J and Brady R: Purification and properties of the major isozymes of α-galactosidase from human placenta. *Journal of Biological Chemistry* 253:184,1978.

17. Salvayre R, Maret A and Douste-Blazy L: Properties of multiple forms of α-galactosidase and α-N-acetylgalactosaminidase from normal and Fabry leukocytes. *European Journal of Biochemistry* 100:377,1979.

18. Salvayre R, Negre A, Maret A, Lenoir G and Douste-Blazy L: Separation and properties of molecular forms of α-galactosidase and α-N-acetylgalactosaminidase from blood lymphocytes and cell lines transformed by epstein-barr virus. *European Journal of Biochemistry* 659:445,1981.

19. Dean KJ and Sweely CC: Studies on human liver α-galactosidases. I. Purification of α-galactosidase A and its enzymatic properties with glycolipid and oligosaccharide substrates. *Journal of Biological Chemistry* 254:10001,1979.

20. Ho M, Beutler E, Tennant L and O'Brien J: Fabry's disease: evidence for a physically altered α-galactosidase *American Journal of Human Genetics* 24:256,1972.

21. Mapes C and Sweely C: Interconversion of the A and B forms of ceramide trihexosidase from human plasma. *Archives of Biochemistry and Biophysics* 158:297,1973.

22. DeGroot PG, Westerveld A, Meera Khan P and Tager JM: Localization of a gene for human alpha-galactosidase B (=N-acetyl-alpha-D-galactosaminidase) on chromosome 22. *Human Genetics* 44:305,1978.

23. Desnick RJ, Bernstein HS, Astrin KH, Potluri VR and Bishop DF: Molecular studies of Fabry disease. *Clinical Research* 34:717A,1986.

24. Bernstein HS, Bishop DF, Astrin KH, Kornreich R, Eng CM, Sakuraba H and Desnick RJ: Fabry disease: six gene rearrangements and an exonic point mutation in the α-galactosidase gene. *Journal of Clinical Investigation* 83:1390,1989.

25. Romeo G, D'Urso M, Pisacane A, Blum E, DeFalco A and Ruffilli A: Residual activity of α-galactosidase A in Fabry's disease. *Biochemical Genetics* 13:615,1975.

26. Kobayashi T, Kira J, Shinnoh N, Goto I and Kuroiwa Y: Fabry's disease with partially deficient hydrolysis of ceramide trihexoside. *Journal of Neurological Science* 67:179,1985.

27. Bach G, Rosenmann E, Karni A and Cohen T: Pseudodeficiency of α-galactosidase A. *Clinical Genetics* 21:59,1982.

28. Bishop DF, Grabowski GA and Desnick RJ: Fabry disease: An asymptomatic hemizygote with significant residual α-galactosidase A activity. *American Journal of Human Genetics* 33:71A,1981.

29. Clarke JTR, Knaack J, Crawhall JC and Wolfe LS: Ceramide trihexosidosis (Fabry's disease) without skin lesions. *New England Journal of Medicine* 284:233,1971.

30. Lemansky P, Bishop DF, Desnick RJ, Hasilik A and von Figura K: Synthesis and processing of α-galactosidase A in human fibroblasts. Evidence for different mutations in Fabry disease. *Journal of Biological Chemistry* 262:2062,1987.

31. Calhoun DH, Bishop DF, Bernstein HS, Quinn M, Hantzopoulos P and Desnick RJ: Fabry disease: isolation of a cDNA clone encoding human α-galactosidase A. *Proceedings of the National Academy of Science USA* 82:7364,1985.

32. Bishop DF, Calhoun DH, Bernstein HS, Hantzopoulos P, Quinn M and Desnick RJ: Human α-galactosidase A: Nucleotide sequence of a cDNA clone encoding the mature enzyme. *Proceedings of the National Academy of Science USA* 83:4859,1986.

33. Bishop DF, Kornreich R and Desnick RJ: Structural organization of the human α-galactosidase A gene: Further evidence for the absence of the 3' untranslated region. *Proceedings of the National Academy of Science USA* 85:3903,1988.

34. Kornreich R, Desnick RJ and Bishop DF: Nucleotide sequence of the human α-galactosidase A gene. *Nucleic Acids Research* 17:3301,1989.

35. Donahue TF: Scanning, internal initiation and the control of the initiation of protein synthesis. *Current Opinion in Cell Biology* 2:1087,1990.

36. Roy A, Chakrabarti D, Datta B, Hileman R and Gupta N: Natural mRNA is required for directing met-tRNA to 40S ribosomal subunits in animal cells: involvement of co-eIF-2A in natural mRNA-directed initiation complex formation. *Biochemistry* 27:8203,1988.

37. Gonsky R, Lebendiker M, Haray R, Banai Y and Kaempfer R: Binding of ATP to eukaryotic initition factor 2. *Journal of Biological Chemistry* 265(16):9083,1990.

38. Rowlands A, Panniers R and Henshaw E: The catalytic mechanism of guanine nucleotide exchange factor and competitive inhibition by phosphorylated eukaryotic initiation factor 2. *Journal of Biological Chemistry* 263:5526,1988.

39. Etchinson D, Milburn S, Edery I, Sonenberg N and Hershey J: Inhibition of HeLa cell protein synthesis following poliovirus infection correlates with the the proteolysis of a 220,000 dalton polypeptide associated with eukaryotic initiation factor 3 and a cap binding complex. *Journal of Biological Chemistry* 257:14806,1982.

40. Sonenberg N, Guertin D and Lee K: Capped mRNA's with reduced secondary structure can function in extracts from poliovirus-infected cells. *Molecular and Cellular Biology* 2:1633,1982.

41. Seal S, Schmidt A and Marcus A: Ribosome binding to inosine-substituted mRNAs in the absence of ATP and mRNA factors. *Journal of Biological Chemistry* 264:7363,1989.

42. Kozak M: Circumstances and mechanisms of inhibition of translation by secondary structure in eukaryotic mRNA's. *Molecular and Cellular Biology* 9:5134,1989.

43. Pelletier J and Sonenberg N: Insertion mutagenesis to increase secondary structure within the 5' noncoding region of a eukaryotic mRNA reduces translational efficiency. *Cell* 40:515,1985.

44. Kozak M: Influences of mRNA secondary structure on initiation by eukaryotic ribosomes. *Proceedings of the National Academy of Science USA* 83:2850,1986.

45. Baim S and Sherman F: mRNA structures influencing translation in the yeast *Saccharomyces cerevisiae*. *Molecular and Cellular Biology* 8:1591,1988.

46. Manzella J and Blackshear P: Regulation of rat ornithine decarboxylase mRNA translation by its 5'-untranslated region. *Journal of Biological Chemistry* 265:11817,1990.

47. Crum C: Complementary oligodeoxy-nucleotide mediated inhibition of tobacco mosaic virus RNA translation *in vitro*. *Nucleic Acids Research* 16:4569,1988.

48. Hassin D, Korn R and Horowitz M: A major internal initiation site for the *in vitro* translation of adenovirus DNA polymerase. *Virology* 155:214,1986.

49. Herman R: Internal initiation of translation of the VSV phosphoprotein mRNA yields a second protein. *Journal of Virology* 58:797,1986.

50. Nagy E, Duncan R, Krell P and Dobos P: Mapping of the large RNA genome segment of infectious pancreatic necrosis virus by hybrid arrest translation. *Virology* 158:211,1987.

51. Pelletier J and Sonenberg N: Internal initiation of translation of eukaryotic mRNA directed by a sequence derived from poliovirus RNA. *Nature* 334:320,1988.

52. Meerovitch K, Pelletier J and Sonenberg N: A cellular protein that binds to the 5'-noncoding region of poliovirus RNA: implications for internal translation initiation. *Genes and Development* 3:1026,1989.

53. Kaminski A, Howell M and Jackson R: Initiation of encephalolomyocarditus virus RNA translation: the authentic initiation site is not selected by a scanning mechanism. *EMBO Journal* 9:3753,1990.

54. Kozak M: Possible role of flanking nucleotides in recognition of the AUG initiator codon by eukaryotic ribosomes. *Nucleic Acids Research* 9:5233,1981.

55. Kozak M: Compilation and analysis of sequences upstream from the translational start site in eukaryotic mRNA's. *Nucleic Acids Research* 12:857,1984.

56. Kozak M: Point mutations define a sequence flanking the AUG codon that modulates translation by eukaryotic ribosomes. *Cell* 44:283,1986.

57. Kozak M: An analysis of 5'-noncoding sequences from 699 vertebrate messenger RNAs. *Nucleic Acids Research* 15:8125,1987.

58. Kozak M: At least six nucleotides preceding the AUG initiator codon enhance translation in mammalian cells. *Journal of Molecular Biology* 196:947,1987.

59. Kozak M: The scanning model for translation: an update. *Journal of Cell Biology* 108:229,1989.

60. Kozak M: A short review of scanning. In: McCarthy JEG, Tuite MF, ed. *Post-Transcriptional Control of Gene Expression* Heidelberg: Springer-Verlag,1990: 227,vol 49.

61. Kozak M: Downstream secondary structure facilitates recognition of initiator codons by eukaryotic ribosomes. *Proceedings of the National Academy of Science USA* 87:8301,1990.

62. Cigan A and Donahue T: Sequence and structural features associated with translational initiation regions in yeast-a review. *Gene* 59:1,1987.

63. Kozak M: Translation of insulin-related polypeptides from mRNA with tandemly reitierated copies of the ribosome binding site. *Cell* 34:971,1983.

64. Mueller P and Hinnebusch A: Multiple upstream AUG codons mediate translational control of GCN4. *Cell* 45:201,1986.

65. Werner M, Feller A, Messenguy F and Pierard A: The leader peptide of yeast CPA1 is essential for translational repression of its expression. *Cell* 49:805,1987.

66. Kozak M: Effects of intercistronic length on the efficiency of reinitiation by eukaryotic ribosomes. *Molecular and Cellular Biology* 7:3438,1987.

67. Mueller P, Jackson B, Miller P and Hinnebusch A: The first and fourth upstream open reading frames in GCN4 mRNA have similar initiation frequencies but respond differently in translational control to changes in length and sequence. *Molecular and Cellular Biology* 8:5439,1988.

68. Williams N, Mueller P and Hinnebusch A: The positive regulatory function of the 5'-proximal open reading frame in GCN4 mRNA can be mimicked by heterologous, short coding sequences. *Molecular and Cellular Biology* 8:3827,1988.

69. Tzamarias D, Roussou I and Thireos G: Coupling of GCN4 mRNA translational activation with decreased rates of polypeptide chain initiation. *Cell* 57:947,1989.

70. Sedman S, Good P and Mertz J: Leader-encoded open reading frames modulate both the absolute and relative rates of synthesis of the virion proteins of Simian Virus 40. *Journal of Virology* 63:3884,1989.

71. Sedman S, Gelembiuk G and Mertz J: Translation initiation at a downstream AUG occurs with increased efficiency when the upstream AUG is located very close to the 5' cap. *Journal of Virology* 64:453,1990.

72. Miller P and Hinnebusch A: Sequences that surround the stop codons of upstream open reading frames inGCN4 mRNA determine their distinct function in translational control. *Genes and Development* 3:1217,1989.

73. Abastado J-P, Miller P, Jackson B and Hinnebusch A: Suppression of ribosomal reinitiation at upsteam open reading frames in amino acid-starved cells forms the basis for GCN4 translational control. *Molecular and Cellular Biology* 11:486,1991.

74. Theil EC: Regulation of ferritin and transferrin receptor mRNAs. *Journal of Biological Chemistry* 265:4771,1990.

75. Kuhn LC: mRNA-protein interactions regulate critical pathways in cellular iron metabolism. *British Journal of Haematology* 79:1,1991.

76. Joshi-Barve S, Rychlik W and Rhoads R: Alteration of the major phosphorylation site of eukaryotic protein synthesis initiation factor 4E prevents its association with the 48S initiation complex. *Journal of Biological Chemistry* 265:2979,1990.

77. Morley SJ and Traugh JA: Differential stimulation of phosphorylation of initiation factors eIF-4F, eIF-4B, eIF-3, and ribosomal protein S6 by insulin and phorbol esters. *Journal of Biological Chemistry* 265:10611,1990.

78. Lazaris-Karatzas A, Montine K and Sonenberg N: Malignant transformation by a eukaryotic initiation factor that binds to mRNA 5' cap. *Nature* 345:544,1990.

79. Duncan R and Hershey JWB: Heat shock-induced translational alterations in HeLa cells. *Journal of Biological Chemistry* 259:11882,1984.

80. Duncan R and Hershey JWB: Initiation factor protein modifications and inhibitions of protein synthesis. *Molecular and Cellular Biology* 7:1293,1987.

81. Trachsel H and Staehelin T: Binding and release of eukaryotic initiation factor eIF-2 and GTP during protein synthesis initiation. *Proceedings of the National Academy of Science USA* 75:204,1978.

82. Pathak V, Schindler D and Hershey J: Generation of a mutant form of protein synthesis initiation factor eIF-2 lacking the site of phosphorylation by eIF-2 kinases. *Molecular and Cellular Biology* 8:993,1988.

83. Pain VM: Initiation of protein synthesis in mammalian cells. *Biochemical Journal* 235:625,1986.

84. Colthurst D, Cambell D and Proud C: Structure and regulation of initiation factor eIF-2. *European Journal of Biochemistry* 166:357,1987.

85. Dholakia JN and Wahba AJ: Phosphorylation of the guanine nucleotide exchange factor from rabbit reticulocytes regulates its activity in polypeptide chain initiation. *Proceedings of the National Academy of Sciences USA* 85:51,1988.

86. Munroe D and Jacobson A: mRNA poly(A) tail, a 3' enhancer of translational initiation. *Molecular and Cellular Biology* 10:3441,1990.

87. Sachs A and Davis R: The poly(A) binding protein is required for poly(A) shortening and 60S ribosomal subunit-dependent translation initiation. *Cell* 58:857,1989.

88. Jackson R and Standart N: Do the poly(A) tail and 3' untranslated region control mRNA translation? *Cell* 62:15,1990.

89. Drummond D, Armstrong J and Coleman A: The effect of capping and polyadenylation on the stability, movement and translation of synthetic messenger RNAs in *Xenopus* oocytes. *Nucleic Acids Research* 13:7375,1985.

90. Galili G, Kawata E, Smith L and Larkins B: Role of the 3'-poly(A) sequences in translational regulation of mRNAs in *Xenopus laevis* oocytes. *Journal of Biological Chemistry* 263:5764,1988.

91. Richter JD: Molecular mechanisms of translational control during the early development of *Xenopus laevis*. In: Ilan J, ed. *Translational Regulation of Gene Expression* New York: Plenum Publishing Corporation, 1987: 111.

92. Fu L, Ye R, Browder L and Johnston R: Translational potential of messenger RNA with secondary structure in Xenopus. *Science* 251:807,1991.

93. Mariottini P and Amaldi F: The 5' untranslated region of mRNA for ribosomal protein S19 is involved in its translational regulation during *Xenopus* development. *Molecular and Cellular Biology* 10:816,1990.

94. Cordell B, Diamond D, Punter J, Schone H and Goodman H: Disproportionate expression of the two nonallelic rat insulin genes in a pancreatic tumor is due to translational control. *Cell* 31:531,1982.

95. Endo T and Nadal-Ginard B: Three types of muscle-specific gene expression in fusion-blocked rat skeletal muscle cells: translational control in EGTA-treated cells. *Cell* 49:515,1987.

96. Johnson DL and Desnick RJ: Physical and kinetic properties of α-galactosidase A in cultured human endothelial cells. *Biochemica et Biophysica Acta* 538:195,1978.

97. Bishop DF and Desnick RJ: Affinity purification of α-galactosidase A from human spleen, placenta, and plasma with elimination of pyrogen contamination. Properties of the purified splenic enzyme compared to other forms. *Journal of Biolological Chemistry* 256:1307,1981.

98. Dawson G, Matalon R and Li YT: Correction of the enzymatic defect in cultured fibroblasts from patients with Fabry's disease: Treatment with purified α-galactosidase from Ficin. *Pediatric Research* 7:694,1973.

99. Mapes CA, Anderson RL, Desnick RJ, Krivit W and Sweeley CC: Enzyme replacement as a possible therapy for Fabry's disease. *Science* 169:987,1970.

100. Desnick RJ, Dean KJ, Grabowski G, Bishop DF and Sweeley CC: Enzyme therapy in Fabry disease: Differential *in vivo* plasma clearance and metabolic effectiveness of plasma and splenic α-galactosidase A isozymes. *Proceedings of the National. Academy of Science USA* 76:5326,1979.

101. Elleder M, Bradova V and Smid F: Cardiocyte storage and hypertrophy as a sole manifestation of Fabry's disease. *Virchows Archiv A* 417:449,1990.

102. Ogawa K, Sugamata K and Funamoto N: Restricted accumulation of globotriaosylceramide in the hearts of atypical cases of Fabry's disease. *Human Pathology* 21:1067,1990.

103. von Scheidt W, Eng CM, Fitzmaurice TF, Erdman E, Hubner G, Olsen EGJ, Christomanou H, Kandolph R, Bishop DF and Desnick RJ: An atypical variant of Fabry's disease with manifestations confined to the myocardium. *New England Journal of Medicine* 324:395,1991.

104. Desnick RJ, Allen KY, Desnick SJ, Raman MK, Bernlohr RW and Krivit W: Fabry disease: Enzymatic diagnosis of hemizygotes and heterozygotes. α-Galactosidase activities in plasma, serum, urine and leukocytes. *Journal of Laboratory Clinical Medicine* 81:157,1973.

105. Gomori G: Preparation of buffers for enzyme studies. In: *Methods in Enzymology* vol 1:138, 1955.

106. Bishop D and Desnick R: Affinity purification of α-galactosidase A from human spleen, placenta, and plasma with elimination of pyrogen contamination. *Journal of Biological Chemistry* 256:1307,1981.

107. Dixon M and Webb E: In *Enzymes* (Third ed.) New York: Academic Press, 1979

108. Chirgwin JM, Przybyla AE, MacDonald RJ and Rutter WJ: Isolation of biologically active ribonucleic acid from sources enriched in ribonuclease. *Biochemistry* 18:5294,1979.

109. Chen C and Okayama H: High-efficiency transformation of mammalian cells by plasmid DNA. *Molecular and Cellular Biology* 7:2745,1987.

110. Nishikawa K: Assesment of secondary-structure prediction of proteins. Comparison of computerized Chou-Fasman method with others. *Biochimica et Biophysica Acta* 748:285,1983

111. Kabsch W and Sander C: How good are predictions of protein secondary structure? *FEBS Letters* 155:179,1983.

112. Sakuraba H, Oshima A and Fukuhara Y: Identification of point mutations in the α-galactosidase A gene in classical and atypical hemizygotes with Fabry disease. *American Journal of Human Genetics* 47:784,1990.

113. Higuchi R: Rapid, efficient DNA extraction for PCR from cells or blood. *Amplifications* May:1,1989.

114. Bishop DF, Kornreich R, Eng CM, Ioannou YA, Fitzmaurice TF and Desnick RJ: Human α-galactosidase: Characterization and eukaryotic expression of the full-length cDNA and structural organization of the gene. In: Salvayre R, Douste-Blazy L, Gatt S, ed. *Lipid Storage Disorders* New York: Plenum, 1988: 809.

115. Zuker M: On finding all suboptimal foldings of an RNA molecule. *Science* 244:48,1989.

116. Kozak M: Influence of mRNA secondary structure on binding and migration of 40S ribosomal subunits. *Cell* 19:79,1980.